LBL-22998

Lawrence Berkeley Laboratory
UNIVERSITY OF CALIFORNIA

APR 22 1987

To be published as a chapter in
Charged Particle Emission from Nuclei,
Vol. II, M. Ivascu and D. Poenaru, Eds.,
CRC Press, Cleveland, OH, 1987

BETA-DELAYED TWO-PROTON EMISSION

D. Moltz and J. Cerny

February 1987

TWO-WEEK LOAN COPY
This is a Library Circulating Copy which may be borrowed for two weeks.

NUCLEAR SCIENCE DIVISION

LBL-22998

Prepared for the U.S. Department of Energy under Contract DE-AC03-76SF00098

DISCLAIMER

This document was prepared as an account of work sponsored by the United States Government. While this document is believed to contain correct information, neither the United States Government nor any agency thereof, nor the Regents of the University of California, nor any of their employees, makes any warranty, express or implied, or assumes any legal responsibility for the accuracy, completeness, or usefulness of any information, apparatus, product, or process disclosed, or represents that its use would not infringe privately owned rights. Reference herein to any specific commercial product, process, or service by its trade name, trademark, manufacturer, or otherwise, does not necessarily constitute or imply its endorsement, recommendation, or favoring by the United States Government or any agency thereof, or the Regents of the University of California. The views and opinions of authors expressed herein do not necessarily state or reflect those of the United States Government or any agency thereof or the Regents of the University of California.

LBL-22998

Beta-Delayed Two-Proton Emission

D.M. Moltz and J. Cerny

Nuclear Science Division
Lawrence Berkeley Laboratory
University of California
Berkeley, California 94720

This work was supported by the Director, Office of Energy Research, Division of Nuclear Physics of the Office of High Energy and Nuclear Physics of the U.S. Department of Energy under Contract DE-AC03-76SF00098.

Beta-Delayed Two-Proton Emission

D. M. Moltz and Joseph Cerny, Department of Chemistry and Lawrence Berkeley Laboratory, University of California, Berkeley, CA 94720 USA

Introduction

Proton rich nuclei have always proven to be an excellent source of exotic decay modes. Although standard β^+ and alpha-particle decay have long been decay measurement standards, beta-delayed particle emission has become a preferred probe as experiments proceed further from stability. Beta-delayed proton emission has ceased to be considered a particularly exotic decay mode simply because there are now in excess of 75 isotopes which exhibit this phenomenon. It still, however, remains an extremely sensitive nuclear structure probe. Beta-delayed alpha-particle emission is not nearly as prevalent as beta-delayed proton emission in spite of the excellent stability of the alpha particle. As experiments extend toward the proton drip-line, additional exotic decay modes (proton radioactivity, two-proton radioactivity, and beta-delayed two-proton radioactivity) are predicted to dominate. Primarily due to experimental accessibilty, much of this work has been concentrated in the light proton-rich nuclei (see ref. 1 for a general review).

These exotic decay modes were in general predicted many years ago. Ground state proton emission [2,3] and ground state two-proton emission [4,5]

have been predicted since 1914 and 1960, respectively. Although direct proton emission was first observed from a $19/2^-$ isomer in ^{53}Co,[6,7] only recently has it been observed from the ground state. To date only four nuclei have been shown to decay via this mode, ^{151}Lu, ^{147}Tm,[8,9] ^{113}Cs and ^{109}I [10] (but see also ref. 11). Although the appropriate target and projectile combinations have only become more generally available in recent years for the production of these heavy nuclei at the proton drip-line, the observations of their decays are facilitated by the long proton half-lives due to the large Coulomb barriers. In light nuclei the Coulomb barriers are very small, thus requiring the observation of low energy (< 500 keV) protons in a nominal half-life range of, say, <1 μs to 10 ms where proton decay would predominate over beta decay. These two experimental regimes are independently difficult to cover, and an approach providing an appropriate combination of the two has yet to be developed. The only exception to these general criteria occurs when a large centrifugal barrier also exists, such as in the decay of $^{53}Co^m$.

The discovery of direct ground state two-proton decay has been hampered by the stringent energetics requirement (unbound to two proton emission but bound to single proton emission) and by the need to detect fairly low energy protons. Although Gol'danskii's prediction of this decay mode was made many years ago,[4,5] he only recently predicted the existence of another exotic decay mode for proton-rich nuclei, that of beta-delayed two-proton emission.[12] The energy requirements for this decay mode are illustrated in Fig. 1 relative to that for beta-delayed single proton emission. For the particular case shown, beta decay of the precursor is shown populating the isobaric analog state in the emitter which then may decay by several (isospin-forbidden) modes.

Such a decay could proceed via several mechanisms: sequential emission or direct emission of either a correlated (^{2}He) or uncorrelated pair of protons. These decay mechanisms would generate vastly different experimental signatures. Monte Carlo simulations depicted in Fig. 2 and Fig. 3 show the primary differences between the first two mechanisms.[13] (The decay example used is the decay of ^{22}Al (see below) via the isobaric analog state in ^{22}Mg to the first excited state of ^{20}Ne.) Figure 2 illustrates that coincidence experiments involving sequential decay would detect a proton of unique energy and a proton whose laboratory energy would depend upon the relative angle of observation. This kinematic effect would also cause the observed peak for the second proton to broaden over the finite set of observable angles. The angular correlation for a sequential decay process would depend upon the angular momentum of the initial, intermediate and final states. For many cases, anisotropies of only 10-20% are expected. This differs markedly from the observations one would expect for ^{2}He emission from the analog state in light nuclei illustrated in Fig. 3. In this case a very sharp 2p peak would in principle be observable, dependent only upon the widths of the nuclear states (which should be very small for the isobaric analog state shown in Fig. 1) and the detector resolutions. However, the individual proton energies would consist of a continuum centered at $E_{p1} = E_{p2}$. The lower yield at equal energies is due to the final state interaction of the two protons, as observed in reaction studies.[14,15] This interaction would also serve to peak the angular distribution around 30° for this example, with no protons observed beyond ~70°. Finally, emission of an uncorrelated pair of protons should yield an isotropic angular distribution with an energy continuum. More details of these Monte Carlo simulations may be found elsewhere.[13]

Discovery of Beta-Delayed Two-Proton Emission

Gol'danskii [12] had predicted that the odd-odd, A = 4n+2, T_z = -2 nuclides should be good candidates for beta-delayed two-proton emission. Earlier beta-delayed proton studies on the A = 4n, T_z= -2 nuclei, ^{32}Ar,[16] ^{20}Mg,[17] ^{24}Si [18] and ^{36}Ca,[19] had required mass separation from the copiously and simultaneously produced A = 4n+1, T_z = -3/2 series of strong beta-delayed proton emitters. However, the odd-odd T_z = -2 nuclei have very large Q_β values with equivalently large energies available for proton (and two-proton) decay from the isobaric analog state in the daughter nucleus. Thus mass separation was not essential. By utilizing the helium-jet recoil transport method in conjunction with a slowly rotating catcher wheel and a standard ΔE-E silicon detector telescope depicted in Fig. 4, the beta-delayed proton decay of the lightest bound member of this series, ^{22}Al, was observed.[20] Figure 5 shows the results of the 60 and 110 MeV ^{3}He + Mg bombardments. The identification of the proton groups labeled "^{22}Al" in Fig. 5(b) are based on predicted energies and the known difference of the energies of the final states in ^{21}Na. Also, the below-threshold bombardment shown in Fig. 5(a) did not show any sign of these groups. The decay scheme (shown in Fig. 13 following) features one of the highest observed beta-decay energies for proton-rich nuclei, being nearly twice that of the even-Z, T_z = -2 nuclei. The success of this experiment then led to the discovery of the next member of this series, ^{26}P,[21] using the same experimental conditions with a Si target.

^{22}Al was predicted to be unstable with respect to two-proton emission from the isobaric analog state of its beta daughter. In order to search for this new decay mode, the experimental setup depicted in Fig. 6 was constructed. The most important addition to existing equipment was the manufacture of two diffused junction silicon detectors on a single wafer by dividing the circular surface contact on one side on the centerline. Both the ΔE_1 (20-40 μm) and ΔE_2 (100-400 μm) detectors were of this type. The E counter was a single detector ~1000 μm thick. This "narrow angle" setup subtended laboratory angles of ~0-70° with a weighted average of 45°; this angular range could observe events independent of the decay mechanism. Figure 7 shows the 2p summed spectrum[13] collected following the bombardment of a natural Mg target by 2.30 C of 110 MeV $^3He^{2+}$ beam from the Lawrence Berkeley Laboratory's 88-Inch Cyclotron. Such studies of ^{22}Al represent the discovery of beta-delayed two-proton emission.[22] The peaks labeled "g" and "x" refer to the ground state and first excited state in the 2p daughter, ^{20}Ne. The individual protons associated with these two peaks are also shown in Fig. 7 and at least in first order suggest a sequential decay mechanism.

To evaluate the mechanism, the "wide angle" setup shown in Fig. 8 was constructed; here the angular range subtended was 70-170°. Figure 9 shows the results of the 110 MeV $^3He^{2+}$ + Mg bombardment for 1.13 C.[13] The same "g" and "x" peaks were observed, only this time they were broader and shifted to higher energies. This is much more apparent in Fig. 10 where the wide angle and narrow angle data have been superimposed. This energy difference can be attributed solely to the kinematic shift between the 45° and 120° average angles. Calculating this

energy difference is relatively straightforward utilizing standard kinematic formulae. These equations have been summarized elsewhere.[13]

There exist two puzzles about the ^{22}Al data which remain unresolved. The first involves the individual proton energy spectra shown in Fig. 7 and Fig. 9. If one compares the protons arising from the "x" peak at wide and narrow angles, there seems to be a reasonable qualitative agreement (general shape and intensities). However, a similar comparison between the wide and narrow angle data for the "g" peak shows a striking difference in the peaks labeled "g1" and "g1' ". These peaks are substantially more intense at wide angles than would be expected. The second puzzle is the change of 2p/1p branching ratio for ^{22}Al decay from 5.5 when observed at large angles to 1.9 at small angles.[13]

After characterizing ^{22}Al, the possible decay via beta-delayed two-proton emission of the next higher A= 4n+2, T_z = -2 nuclide was also investigated. A two-proton sum spectrum arising from a 110 MeV ^{3}He + Si bombardment for 0.60 C is shown in Fig. 11.[23] These data were acquired with the narrow angle setup described previously. Figure 12 shows data collected with the wide angle setup for 1.73 C.[13] The simultaneous production of ^{22}Al provided a calibration, and the new peaks could be readily attributed to ^{26}P. It is interesting to note that decay by correlated 2p (^{2}He) emission from the 3^{+} isobaric analog state in ^{26}Si to the ground state of ^{24}Mg is spin-parity forbidden. The apparent sequential nature of the decay can be established through the individual proton spectra at the two angles given in Fig. 11 and Fig. 12.

With both beta-delayed single proton and two-proton data available, the decay schemes for ^{22}Al and ^{26}P shown in Fig. 13(a,b) can be constructed. Clearly, the discovery of beta-delayed two-proton emission provides a unique spectroscopic tool for studying certain nuclei near the proton drip-line,particularly when mass separation is impractical and when competing reactions which produce strong beta-delayed proton emitters prevent the identification of new single beta-delayed proton emitting isotopes. Additionally, a new and interesting decay mechanism warranted further study. Both of these applications will be addressed in following sections.

Decay Mechanism

As noted earlier, beta-delayed two-proton decay can proceed by either the sequential emission or by the correlated or uncorrelated simultaneous emission of two protons. Of particular interest would be the case of two correlated protons in a relative $^1S_0$ configuration (^2He). This would comprise a unique decay mode, permitting studies of how such a pair of particles would traverse the Coulomb and centrifugal barriers.[14,15] Since, as noted above, the observed 2p decay for ^{26}P cannot occur via this mode,[23] additional decay mechanism studies [24] have been performed on ^{22}Al. The setup used is shown in Fig. 14 and is identical to that used in the wide angle measurements [13] (see Fig. 8) except for the ΔE_2 detectors; these were replaced with position sensitive detectors. The position sensitive direction was aligned such that the relative angle between the two protons could be determined to a few degrees. The efficiency for such a setup peaks at the midpoint angle (120° in this case) and declines

linearly to zero at the extreme angles. After correcting the data with this efficiency curve, the larger angle part of the angular distribution shown in Fig. 15 was obtained, which is consistent with an isotropic distribution.

In a related measurement,[24] a highly collimated narrow angle setup was used to limit the angular range, thereby obtaining a small angle data point. Because of the severe collimation needed to restrict the angular acceptance, the event rate was so small that it permitted the measurement of only the single data point shown in Fig. 15, around 25°. The error bars on this measurement were sufficiently large that an admixture of ^{2}He emission could not be excluded. The dashed curve in Fig. 15 represents an angular distribution calculated with the inclusion of a 15% ^{2}He emission taken from reaction studies.[14,15] Clearly, a higher statistics measurement would be of interest. Although non-sequential decay processes are a possibility in higher mass, proton-rich precursors, the larger Coulomb barrier associated with their decay via this mode may well preclude their occurrence.

Discovery of New Nuclides

Beta-delayed two-proton emission provides a unique and powerful tool in the identification and study of very proton rich nuclides. By combining new experimental results such as decays of the isobaric analog state in the beta daughter, with proven theoretical estimates of the appropriate mass excesses, quite reliable assignments of observed radioactivities can be made. For example, a set of mass relations can be generated for proton-rich nuclei from the approach of Kelson and Garvey[25] which symmetrically utilizes masses across the Z=N line. One generalized

version for the mass difference between mirror nuclides with $T_z = -T$ and $+T$ can be written as:

$$M(A,T_z=-T) - M(A,T_z=+T) = \sum_{A'=A-(2T-1)}^{A+(2T-1)} \left(M(A',-1/2) - M(A',1/2) \right) \qquad (1)$$

Relation (1) can be used to predict the mass of a proton-rich nuclide with $T_z = -T$ from the known masses of the appropriate $T = 1/2$ mirror pairs as well as the mass of its $T_z = +T$ mirror nucleus with typically <300 keV errors.

Isobaric multiplets also play a significant role in predicting masses of highly proton-rich light nuclides. The masses of analog states in an isospin multiplet can be given by a relationship quadratic in T_z, introduced by Wigner in 1957 as follows:[26]

$$M(A,T,T_z) = a(A,T) + b(A,T)\, T_z + c(A,T)\, T_z^2 \,. \qquad (2)$$

This isobaric multiplet mass equation (IMME) arises via first order perturbation theory from the assumptions that the wave functions of the members of an isospin multiplet are identical and that only two-body forces are responsible for charge dependent effects in nuclei. Possible deviations from this quadratic form can be due to higher order Coulomb or other charge dependent effects as well as to various isospin mixing effects.[27] Both of these approaches to mass prediction have been utilized in analysis following the discovery of the first known stable $T_z = -5/2$ nuclide, ^{35}Ca, via its beta-delayed two-proton decay channel.[28]

Subsequently, three additional T_z = -5/2 nuclides (^{23}Si, ^{27}S and ^{31}Ar) have been discovered to exist [29] (though only the beta-delayed proton decay of ^{31}Ar has been observed to date).[30] (NOTE TO EDITORS: A brief half-page note will be added in proof here on the most recent GANIL results.)

In order to produce ^{35}Ca, the 135 MeV ^{3}He + Ca reaction was employed. The produced nuclides were transported via a helium-jet to the narrow angle detection setup shown in Fig. 6 for observation. (In this case, ^{22}Al β-2p activity was used for calibration.) Figure 16 shows the results of a 2.1 C bombardment. The assignment of the two observed peaks to the decay of ^{35}Ca was predicated on many pieces of information. First, the predicted location of the "G" peak (indicated by the arrow in Fig. 16(a)) agrees extremely well with the observed peak. Second, the energy difference between the "G" and "X" peaks agrees with the known ground state-first excited state energy difference in the 2p daughter, ^{33}Cl. Third, although the "G" peak is extremely close to the ^{22}Al "x" peak in energy (see Fig. 7), ^{22}Al could be ruled out as a source of this radioactivity because a) an X-ray fluorescence measurement of the calcium target found no magnesium impurity (<0.1%) and b) the ^{35}Ca "X" peak had not been observed in prior experiments which produced ^{22}Al. Fourth, the only other proton bound nuclide predicted to decay via β-2p emission that could be produced in this reaction is ^{31}Ar. However, noble gases are not collected by the helium-jet technique. Finally, the individual proton spectra shown in Fig. 16(b) and (c) associated with the "G" and "X" peaks shown in Fig. 16(a) exhibit a peak at almost exactly the same energy. All of this information has been interpreted as evidence for the observation of

the decay of ^{35}Ca. Since the individual proton data in Fig. 16 (b) and (c) suggest a sequential emission, a rudimentary decay scheme shown in Fig. 17 can be constructed (this also uses the average detection angle of 33° derived from the ^{22}Al data). A total center-of-mass energy of 4311(40) keV was obtained for the two-proton decay of the $(1/2^{+})$ T = 5/2 isobaric analog state in ^{35}K.

Measurement of the mass of the isobaric analog state in ^{35}K could then be used with the mass of the lowest T = 5/2 state in ^{35}S [31] and that for the ground state of the $T_z = 5/2$ nucleus ^{35}P [32] as input data to the isobaric multiplet mass equation to predict the ground state mass of ^{35}Ca. In all cases, deriving the unknown $T_z = -T$ mass requires a knowledge of the b coefficient in the equation

$$M(T_z = -T) = M(T_z = +T) - 2bT_z \quad . \qquad (3)$$

This has been done in two different ways. The more reliable case is the one in which three or more members of the multiplet are known; this permits the direct calculation of all three coefficients in the quadratic IMME. Masses calculated via this approach can normally be considered very reliable, with quite low predicted errors. For the A = 35, T = 5/2 sextet, it was possible to use the IMME to predict a value of 4453 (60) keV for the ground state of ^{35}Ca.[28]

A second approach can be illustrated by recent calculations of Antony *et al.*[33] They calculate the b coefficient of equation (3) from the following formula:

$$b = \Delta_{nH} - E_c^{(1)} = -720.4\, A^{2/3} + 1808.6 \text{ (keV)} \qquad (4)$$

where Δ_{nH} is the neutron-hydrogen atom mass difference and the vector part of the nuclear Coulomb energy, $E_c^{(1)}$, is derived from a fit to the experimental Coulomb displacement energies for A = 9-60. This relation for b assumes that its value is a constant for all multiplets of a given mass; it then provides a simple way of predicting masses of very proton-rich nuclei up to A = 60. Utilizing this approach to calculate the b coefficient for A = 35, we obtain a value of 4558 (360) keV, in agreement with the IMME value. Finally, the corresponding prediction for the ^{35}Ca mass excess from the Kelson-Garvey [25] relation gives a mass excess of 4777 keV, which differs significantly from the above results, even though the input masses are all known to a few keV or less. This deviation indicates that ^{35}Ca is probably ~300 keV better bound than predicted by the Kelson-Garvey relation which agrees with what appears to be a common result that this relation tends to underpredict the binding of quite proton-rich nuclei.

Although some of the spectroscopic information obtained from beta-delayed two-proton emission may also be obtained from beta-delayed single proton emission, the number of nuclides which undergo βp emission and are simultaneously produced in large quantities often preclude the use of standard techniques such as the helium-jet. Mass separation is, of course, one solution to this problem. However, the lower efficiencies of general purpose mass separators relative to other techniques make the study of nuclides with low production cross sections difficult. Thus β2p emission should certainly be an effective tool for the discovery of nuclei near the proton drip line.

Future Experiments

The characterization of proton-rich light nuclei even further from beta stability will require many new and novel techniques not only to study beta-delayed two-proton emitters, but also for the observation of ground state proton and two-proton radioactivity. The general problems which need to be overcome involve the very small production cross sections, the quite short half-lives and the need, particularly in many higher mass β2p precursors, to detect low proton energies. Solving the first problem will require longer bombarding times and higher beam currents. Addressing the second problem will require new observational techniques. One such approach is the use of recoil spectrometers such as LISE at GANIL.[34] In this type of spectrometer, recoils from higher energy projectile fragmentation reactions are separated from the primary beam and identified. The decays of very short lived nuclei can subsequently be observed following this on-line identification. A different possibility for observing such decays is the use of a very fast rotating catcher wheel, which can measure activities in the 50 μs to 50 ms range.[35] Recoils from compound nucleus reactions are caught in thin aluminum catcher foils inclined at 70° to the incident beam and are rapidly rotated between two large solid angle proton detector telescopes. Recent tests [35] have successfully observed many beta-delayed proton emitters including ^{33}Ar and the beta-delayed two-proton emitter ^{26}P ($t_{1/2}$ = 20 ms). This type of apparatus should also be suitable for the observation of two-proton radioactivity, which will be discussed later.

The last major obstacle is the development of detectors capable of measuring very low energy protons which would be needed to study ground state proton and two-proton radioactivity as well as some β2p emitters in the $f_{7/2}$ shell (e.g., ^{50}Co). One promising avenue is gas-filled avalanche counters operated at very low pressures. In this way the gas signal need only be used for identification , and not for additive energy (ΔE) purposes. This type of gas-filled detector can easily be used with large area silicon counters serving as E detectors.

Finally, the discovery of new beta-delayed two-proton emitters and the possible existence of direct ground state two-proton emission [4,5,36] as a decay mode requires reliable theoretical mass predictions. Use of both the Kelson-Garvey mass relations[25] and where appropriate the IMME [26] in predicting ground state masses have generally yielded good results. In Figures 18(abc)[37] we give a graphical representation of the combined experimental and theoretical one- and two- proton separation energies for T_z = -2, -5/2, and -3 nuclei, respectively. Figure 19 gives a qualitative picture of known proton-rich beta-delayed one- and two-proton emitters in addition to the predictions given quantitatively in Fig. 18. From these predictions, we see that there exist many potential β2p emitters, but fewer candidates for direct ground state two-proton emission. Although ^{19}Mg (S_{2p}= -1170 keV) and ^{31}Ar (S_{2p}= -190 keV) are potential candidates for this decay mode, the most likely candidate appears to be ^{39}Ti (S_{2p}= -790 keV). ^{19}Mg would probably have an extremely short half-life unsuitable for current techniques and ^{31}Ar is probably sufficiently bound that beta decay would predominate (it could still be a β2p emitter). ^{31}Ar has in

fact been observed as a beta-delayed proton emitter in experiments at GANIL using the LISE spectrometer.[30]

Figure 19 also vividly shows that very little is known about the decays of nuclei with $Z > 20$ and $T_z < -1$ (except for the $A = 4n+1$, $T_z = -3/2$ series of beta-delayed proton emitters (see also ref.1)). In many cases the detection of these nuclides and their exotic decay modes will require the development of new experimental techniques. It is clear that the study of these and other very proton rich nuclei at or near the drip line will be the subject of much future investigation.

References

1 Äystö, J. and J. Cerny, to be published in v. 8 of Treatise on Heavy Ion Science, D.A. Bromley, ed., 1987.

2 Marsden, E., Phil. Mag., 27, 824, 1914.

3 Marsden, E., Phil. Mag., 30, 240, 1915.

4 Gol'danskii, V. I., Nucl. Phys., 19, 482, 1960.

5 Gol'danskii, V. I., Usp. Fiz. Nauk., 87, 255, 1965, (Sov. Phys. Usp, 8, 770, 1966).

6 Jackson, K. P., C. U. Cardinal, H. C. Evans, N. A. Jelley, and J. Cerny, Phys. Lett., 33B, 281, 1970.

7 Cerny, J., J. E. Esterl, R. A. Gough, and R. G. Sextro, Phys. Lett., 33B, 284, 1970.

8 Hofmann, S., G. Munzenberg, F. P. Hessberger, W. Reisdorf, J. R. H. Schneider, and P. Armbruster, Z. Phys., A305, 111, 1982.

9 Klepper, O., T. Batsch, S. Hofmann, R. Kirchner, W. Kurzewicz, W. Reisdorf, E. Roeckl, D. Schardt, and G. Nyman, Z. Phys., A305, 125, 1982.

10 Faesterman, T., A. Gillitzer, K. Hartel, P. Kienle, and E. Nolte, Phys. Lett., 137B, 23, 1984

11 Hofmann, S., Y. K. Agarwal, P. Armbruster, F. P. Hessburger, P. O. Larsson, G. Munzenberg, K. Poppensieker, W. Reisdorf, J. R. H. Schneider, and H. J. Schott, In proc. 7th Int. Conf. on Atomic Masses and Fundamental Constants, Darmstadt-Seeheim, W. Germany, 1984, p. 184.

12 Gol'danskii, V. I., Pis'ma Zh. Eksp. Theor. Fiz., 32, 572, 1980, (Sov. Phys. -JETP Lett., 32, 554, 1980).

13 Cable, M. D., J. Honkanen, E. C. Schloemer, M. Ahmed, J. E. Reiff, Z. Y. Zhou, and J. Cerny, Phys. Rev. C, 30, 1276, 1984.

14 Jahn, R., D. P. Stahel, G. J. Wozniak, R. J. de Meijer, and J. Cerny, Phys. Rev. C, 18, 9, 1978.

15 Stahel, D. P., R. Jahn, G. J. Wozniak, and J. Cerny, Phys. Rev. C, 20, 1680, 1979.

16 Hagberg, E., P. G. Hansen, J. C. Hardy, A. Huck, B. Jonson, S. Mattson, H. L. Ravn, P. Tidemand-Petersson, and G. Walter, Phys. Rev. Lett., 39, 792, 1977.

17 Moltz, D. M., J. Aysto, M. D. Cable, R. D. von Dincklage, R. F. Parry, J. M. Wouters, and J. Cerny, Phys. Rev. Lett., 42, 43, 1979.

18 Aysto, J., D. M. Moltz, M. D. Cable, R. D. von Dincklage, R. F. Parry, J. M. Wouters, and J. Cerny, Phys. Lett., 82B, 43, 1979.

19 Aysto, J., M. D. Cable, R. F. Parry, J. M. Wouters, D. M. Moltz, and J. Cerny, Phys. Rev. C, 23, 879, 1981.

20 Cable, M. D., J. Honkanen, R. F. Parry, H. M. Thierens, J. M. Wouters, Z. Y. Zhou, and J. Cerny, Phys. Rev. C, 26, 1778, 1982.

21 Cable, M. D., J. Honkanen, R. F. Parry, S. H. Zhou, Z. Y. Zhou, and J. Cerny, Phys. Lett., 123B, 25, 1983.

22 Cable, M. D., J. Honkanen, R. F. Parry, S. H. Zhou, Z. Y. Zhou, and J. Cerny, Phys. Rev. Lett., 50, 404, 1983.

23 Honkanen, J., M. D. Cable, R. F. Parry, S. H. Zhou, Z. Y., Zhou, and J. Cerny, Phys. Lett., 133B, 146, 1983.

24 Jahn, R., R. L. McGrath, D. M. Moltz, J. E. Reiff, X. J. Xu, J. Aysto, and J. Cerny, Phys. Rev. C, 31, 1576, 1985.

25 Kelson, I., and G. T. Garvey, Phys. Lett., 23, 689, 1966.

26 Wigner, E. P., In Proc. of the Robert A. Welch Foundation Conference on Chemical Research, Houston, 1957, (ed. W. O. Millikan), p. 67, unpublished.

27 Benenson, W. and E. Kashy, Rev. Mod. Phys., 51, 527, 1979.

28 Aysto, J., D. M. Moltz, X. J. Xu, J. E. Reiff, and J. Cerny, Phys. Rev. Lett., 55, 1384, 1985.

29 Langevin, M., A. C. Mueller, D. Guillemaud-Mueller, M. G. Saint-Laurent, R. Anne, M. Bernas, J. Galin, D. Guerreau, J. C. Jacmart, S. D. Hoath, F. Naulin, F. Pougheon, E. Guinious, and C. Detraz, Nucl. Phys., A455, 149, 1986.

30 Pougheon, F., to be published in the Proceedings of the Nuclear Physics Conference, Bormeo, Italy, Jan. 20-24, 1987.

31 Guichard, A., H. Nann and B. H. Wildenthal, Phys. Rev. C, 12, 1109, 1975.

32 Goosman, D. R., and D. E. Alburger, Phys. Rev. C, 6, 820, 1972.
Thorn, C. E., J.W. Olness and E.K. Warburton, Phys. Rev. C, 30, 1442, 1984.
Mayer, W. A., W. Henning, R. Holzwarth, H. J. Korner, G. Korschinek, W. U. Mayer, G. Rosner and H. J. Scheerer, Z. Phys., A319, 287, 1984.
Drumm, P. V., L. K. Fifield, R. A. Bark, M. A. C. Hotchkis and C. L. Woods, to be published.

33 Antony, M.S., B. Britz, and A. Pape, At. Data Nucl. Data Tables, 34, 279, 1986.

34 Saint-Laurent, M. G., To be published in the Proceedings of the XI International Conference on Electromagnetic Isotope Separators and Techniques Related to their Applications, Los Alamos, NM, August 18-22, 1986, GANIL Report p. 86-18.

35 Hotchkis, M., F. Blonnigen, T. Lang, D. Moltz, J. Reiff, X. Xu, and J. Cerny, Bull Am. Phys. Soc., 31, 1234, 1986.

36 Gol'danskii, V. I., Usp. Fiz. Nauk., 141, 715, 1983, (Sov. Phys. Usp., 26, 1112, 1985).

37 Wapstra, A. H., and G. Audi, Nucl. Phys., A432, 1, 1985.

Figure Captions

Figure 1. Generalized decay scheme for a proton-rich nucleus with large Q_{EC}. Decay of the isobaric analog state (IAS) in the emitter nucleus is depicted as open to the p and 2p decay channels.

Figure 2. Monte Carlo simulation of sequential emission of two protons with E_{2p}^{cm} = 4.48 MeV (a predicted ^{22}Al decay) as would be observed with a detector system capable of detecting the two protons with relative angular range of 0-70°.

(a) Two-proton summed energy spectrum.

(b) Individual proton energy spectrum. Peak heights are arbitrarily normalized to lower energy group for display purposes.

Figure 3. Monte Carlo simulation of ^{2}He emission of two protons with E_{2p}^{cm} = 4.48 MeV as would be observed with the same detector system described in Fig. 2.

(a) Two-proton summed energy spectrum.

(b) Individual proton energy spectrum.

Figure 4. Schematic diagram of the helium-jet apparatus. A standard telescope arrangement for detecting beta-delayed protons is shown.

Figure 5. Beta-delayed proton spectra from ^{3}He bombardment at (a) 60 MeV and (b) 110 MeV. The arrows in (b) correspond to the predicted energies for protons decaying from the isobaric analog state in ^{22}Mg to known states in ^{21}Na.

Figure 6. Schematic diagram of the narrow angle detector system. The split detectors are described in the text.

Figure 7. Proton-proton coincidence spectra obtained with the narrow angle detector system following the decay of ^{22}Al. See text and ref. 13.

(a) Two-proton summed energy spectrum. Groups x and g correspond to transitions involving the ^{20}Ne first excited state and ground state, respectively.

(b) Individual proton energy spectrum for protons forming group x in part (a). Primed peaks probably correspond to the first emitted proton.

(c) Individual proton energy spectrum for protons forming group g in part (a). In this case, g1 and g2' correspond to the first emitted protons.

Figure 8. Schematic diagram of the wide angle detector system. In this setup, two separate three-element detector telescopes are used.

Figure 9. Proton-proton coincidence spectra obtained with the wide angle detector system following the decay of ^{22}Al. See Fig. 8.

(a) Two-proton summed energy spectrum. Groups x and g correspond to transitions involving the ^{20}Ne first excited state and ground state, respectively.

(b) Individual proton energy spectrum for protons forming group x in part (a).

(c) Individual proton energy spectrum for protons forming group g in part (a). Here the g1 and g2' peaks correspond to the first emitted protons.

Figure 10. Kinematic shift of ^{22}Al two-proton peaks shown by superimposing Fig. 7a and 9a. Peak heights have been normalized to the "narrow angle" measurement.

Figure 11. Proton-proton coincidence spectra obtained with the narrow angle detector system following the decays of ^{22}Al and ^{26}P produced in the 110 MeV ^{3}He + Si reaction.

(a) Two-proton summed energy spectrum containing both ^{22}Al and ^{26}P groups.

(b) Individual proton energy spectrum for protons from the ^{26}P g group in part (a). This group corresponds to a transition to the ^{24}Mg ground state. The g1' peak corresponds to the first emitted proton.

Figure 12. Proton-proton coincidence spectra obtained with the large angle detector system following decays of ^{22}Al and ^{26}p.

(a) Two-proton summed energy spectrum containing both ^{22}Al and ^{26}P groups.

(b) Individual proton energy spectrum for protons from the ^{26}P g group in part (a). This group corresponds to a transition to the ^{24}Mg ground state. The g1' peak corresponds to the first emitted proton.

Figure 13. Proposed partial decay schemes for (a) ^{22}Al and (b) ^{26}P.

Figure 14. Schematic diagram of the large angle detector system used to measure the relative angles of the two protons in the beta-delayed two-proton decay of ^{22}Al. The sensitive direction of the position sensitive detectors (PSD) lies in the dimension shown.

Figure 15. Normalized angular correlation for the two protons from the beta-delayed two-proton emission of ^{22}Al to the ^{20}Ne first excited state. The dotted line corresponds to a 15% admixture of ^{2}He emission to an otherwise isotropic distribution. See text.

Figure 16. (a) Beta-delayed two-proton sum spectrum of ^{35}Ca. Groups labeled by G and X are related to the two-proton transitions to the ground and first excited states in the daughter nucleus ^{33}Cl. Part of the continuum in the spectra below 3 MeV is due to positron scattering between the detector wafers. Individual proton energy spectra are shown in (b) and (c) corresponding to the ^{35}Ca (G) and (X) 2p peaks, respectively.

Figure 17. Proposed partial decay scheme for the beta-delayed two-proton emission of ^{35}Ca.

Figure 18. One- and two-proton separation energies for a) T_Z=-2; b) T_Z=-5/2; and c) T_Z=-3 nuclides. The symbols in the binding energy plots are as follows: the full black circles mean that the binding energy value is taken from the 1985 Mass Tables,[37] the open circles mean that the value has been calculated with the Kelson-Garvey relation, and the open squares mean that the value is based on the empirical IMME as applied in reference 33. If the two predicted values are within 100 keV, only an open circle is shown.

Figure 19. Chart of the nuclides showing potential beta-delayed (and direct) proton and two-proton emitters in the Z=10 to Z=32 range.

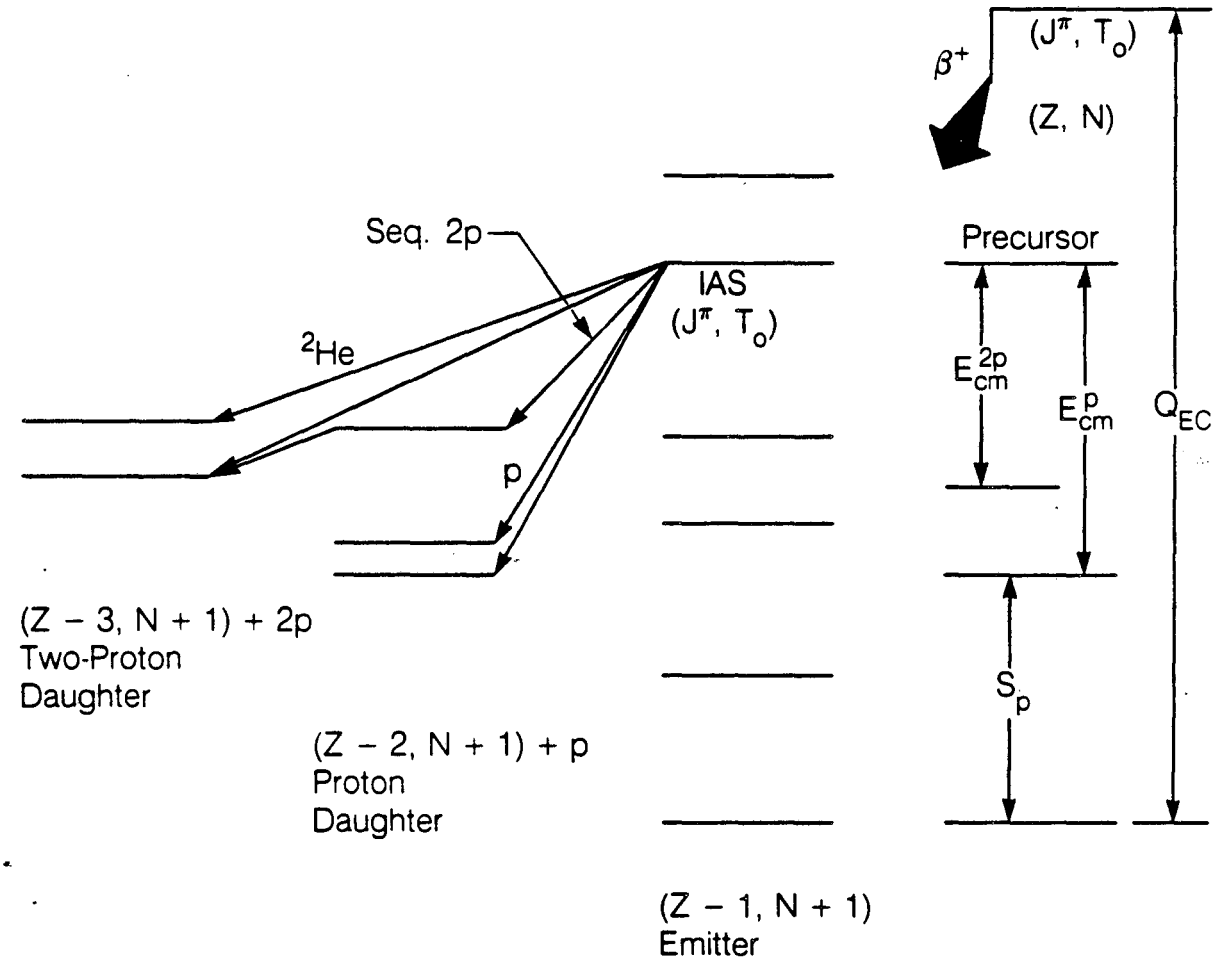

XBL 8612-12850

Figure 1

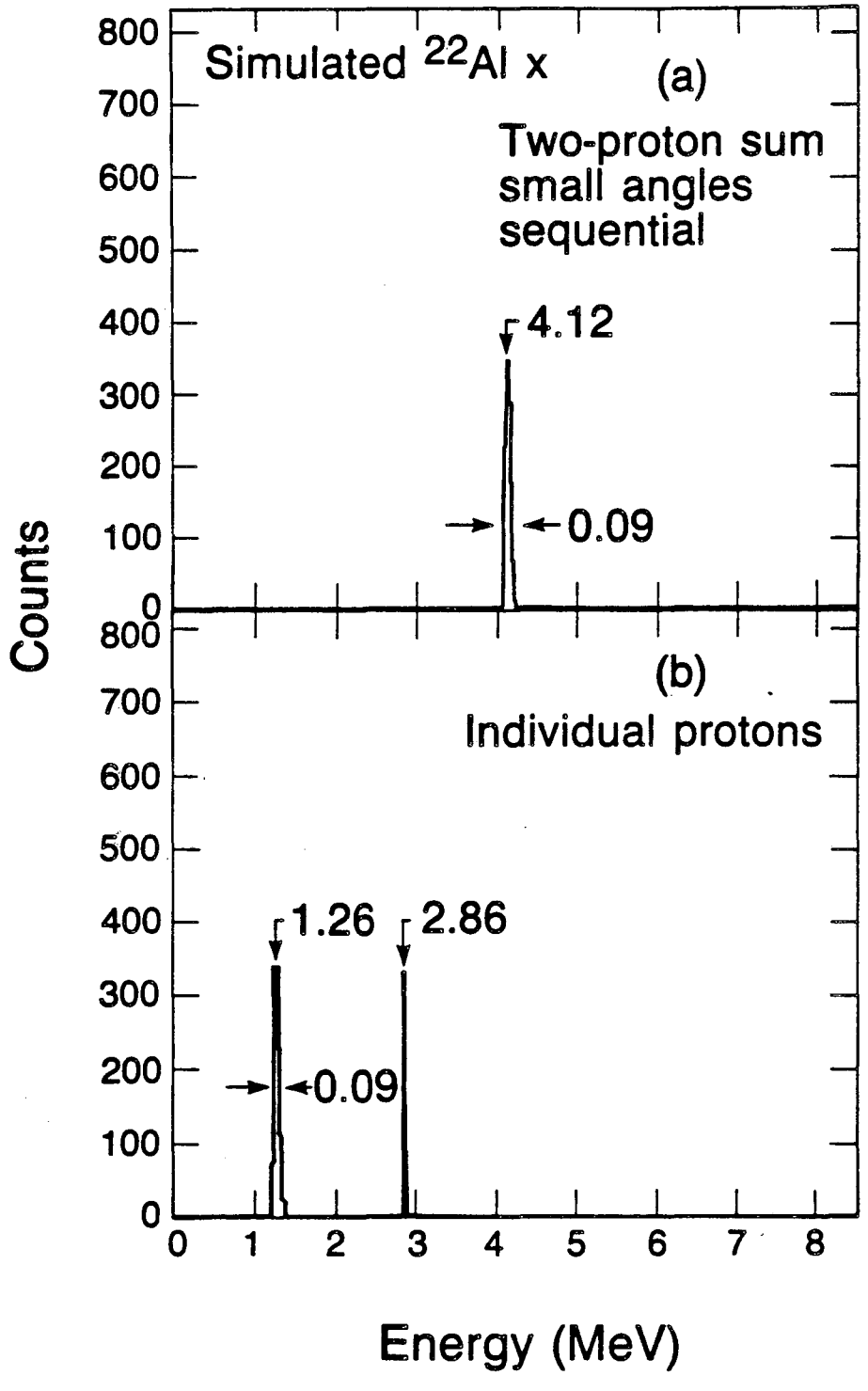

XBL 843-10115

Figure 2

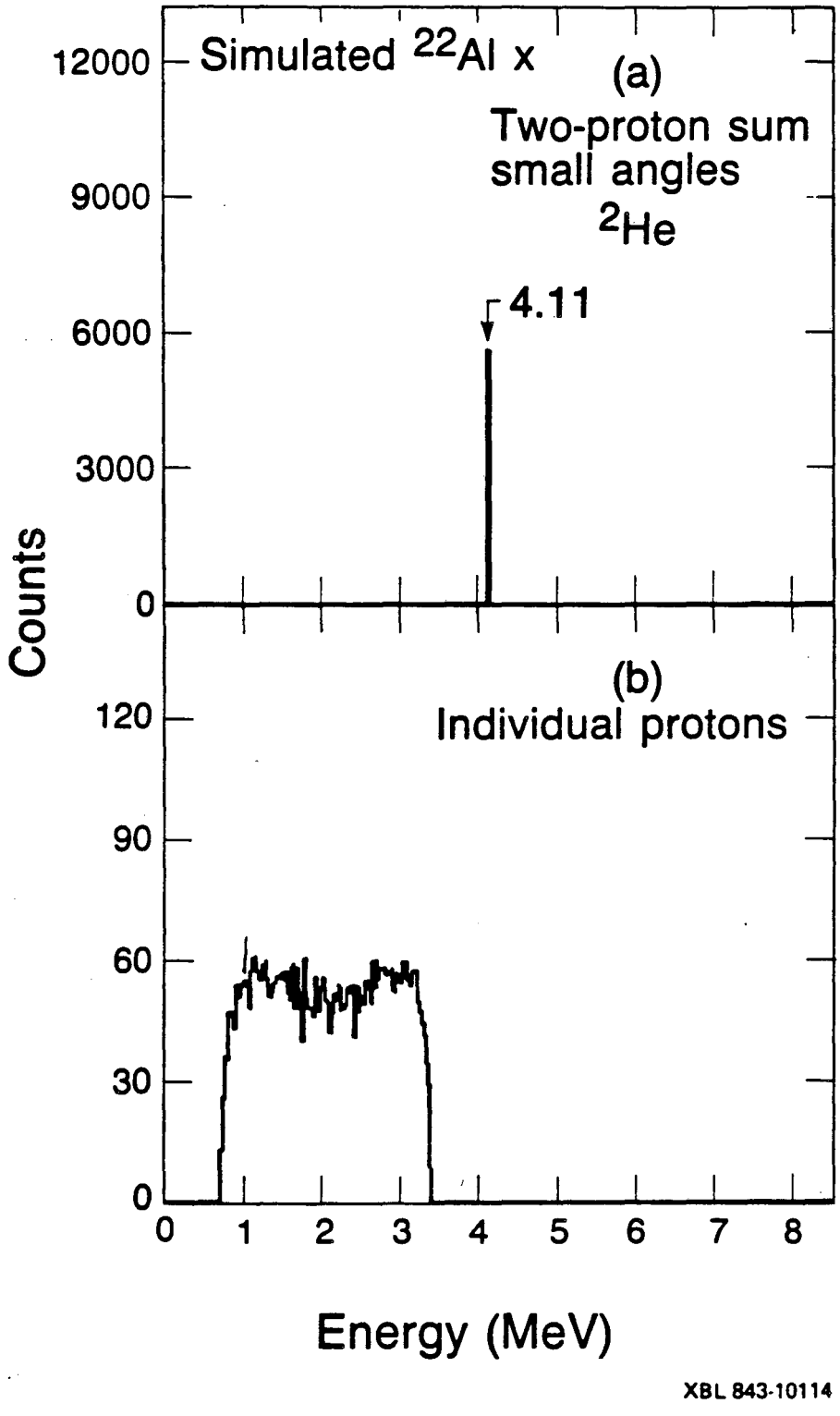
Simulated ^{22}Al x
(a)
Two-proton sum
small angles
^{2}He
4.11
12000
9000
6000
3000
0
Counts
(b)
Individual protons
120
90
60
30
0
0
1
2
3
4
5
6
7
8
Energy (MeV)
XBL 843-10114

Figure 3

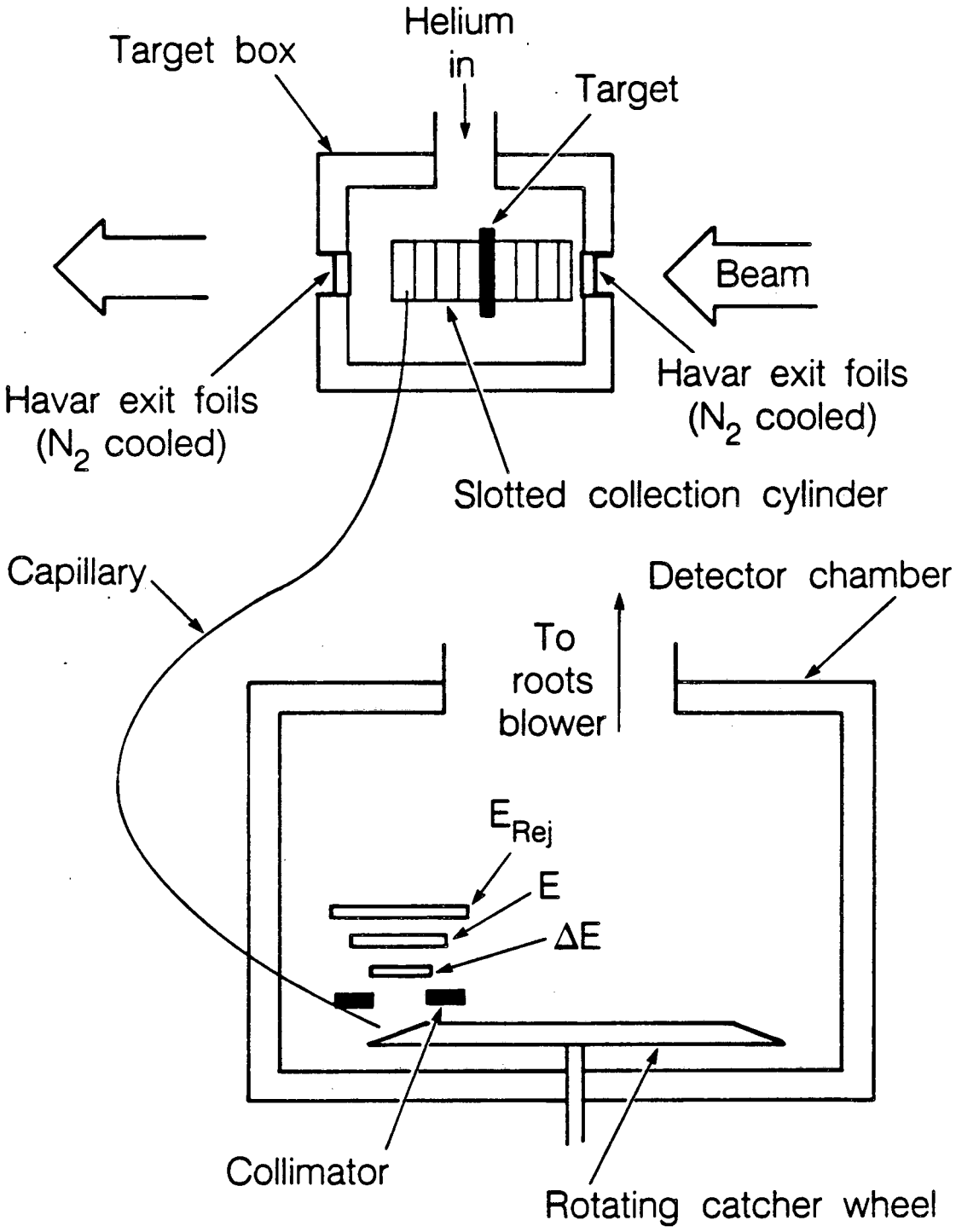

XBL 867-11649

Figure 4

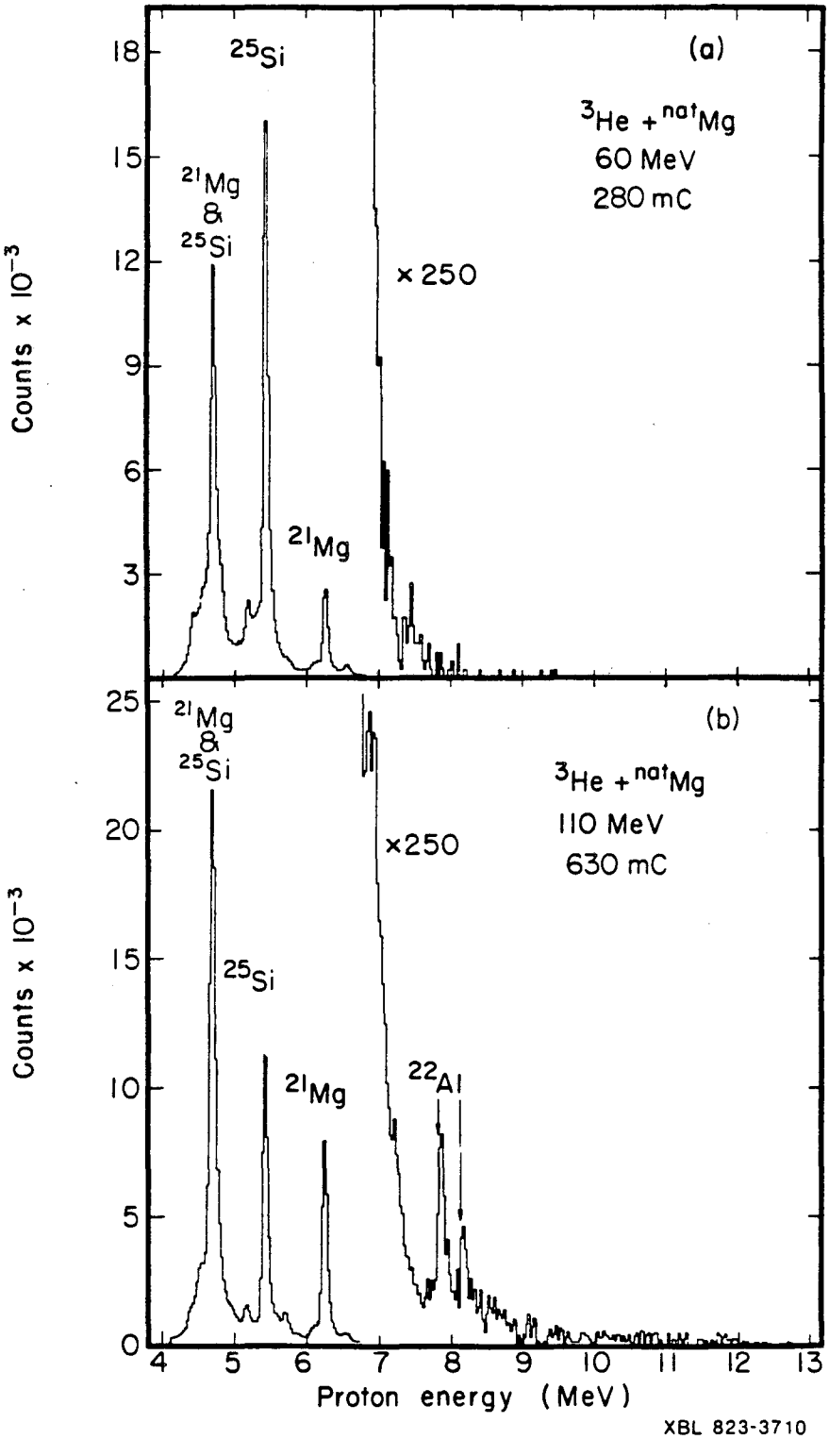
(a)
$^{3}He + ^{nat}Mg$
60 MeV
280 mC
^{25}Si
^{21}Mg & ^{25}Si
^{21}Mg
x 250
(b)
$^{3}He + ^{nat}Mg$
110 MeV
630 mC
^{21}Mg & ^{25}Si
^{25}Si
^{21}Mg
^{22}Al
x250
Counts x 10^{-3}
Proton energy (MeV)
XBL 823-3710

Figure 5

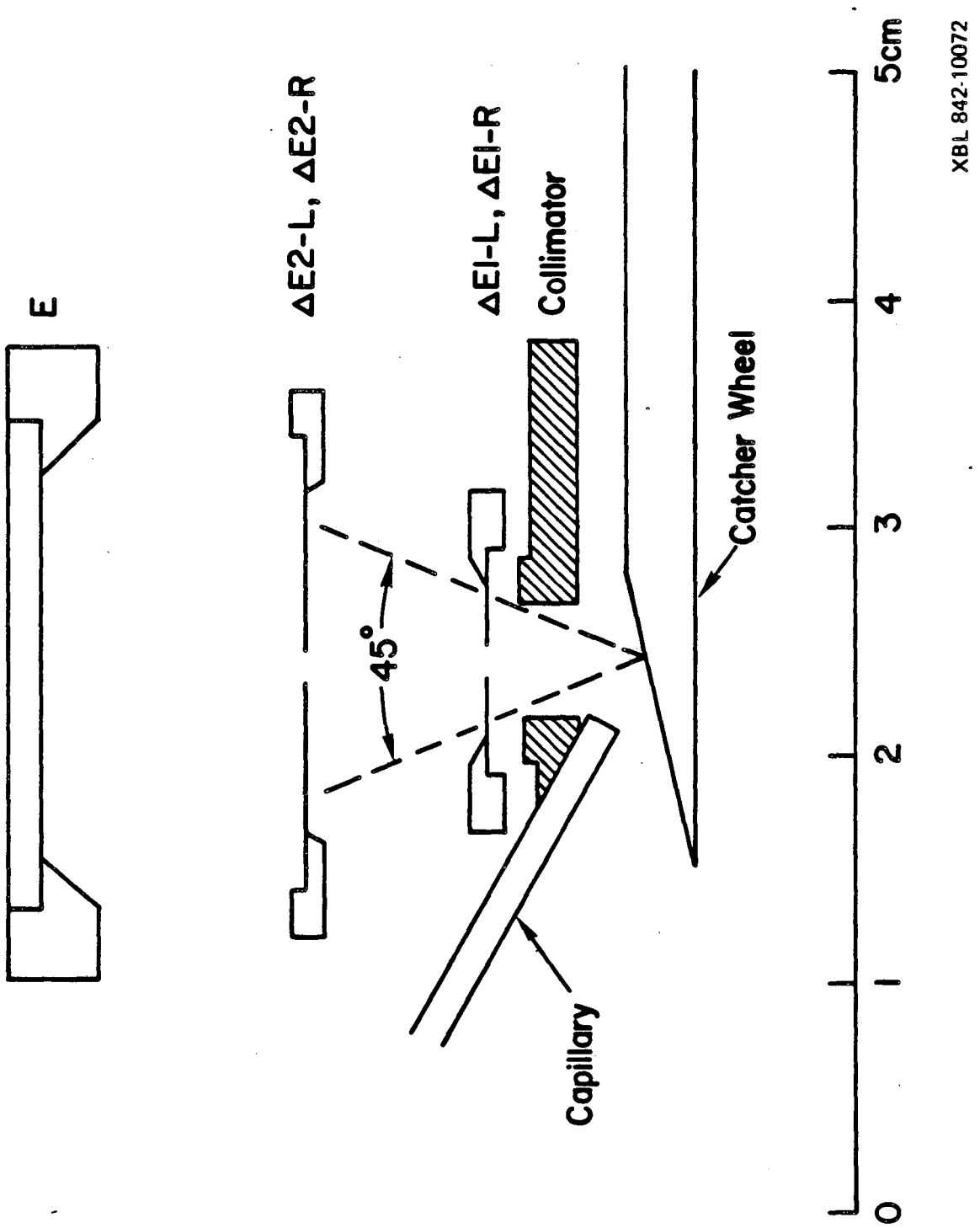
E
ΔE2-L, ΔE2-R
ΔEI-L, ΔEI-R
Collimator
45°
Catcher Wheel
Capillary
0
1
2
3
4
5cm
XBL 842-10072

Figure 6

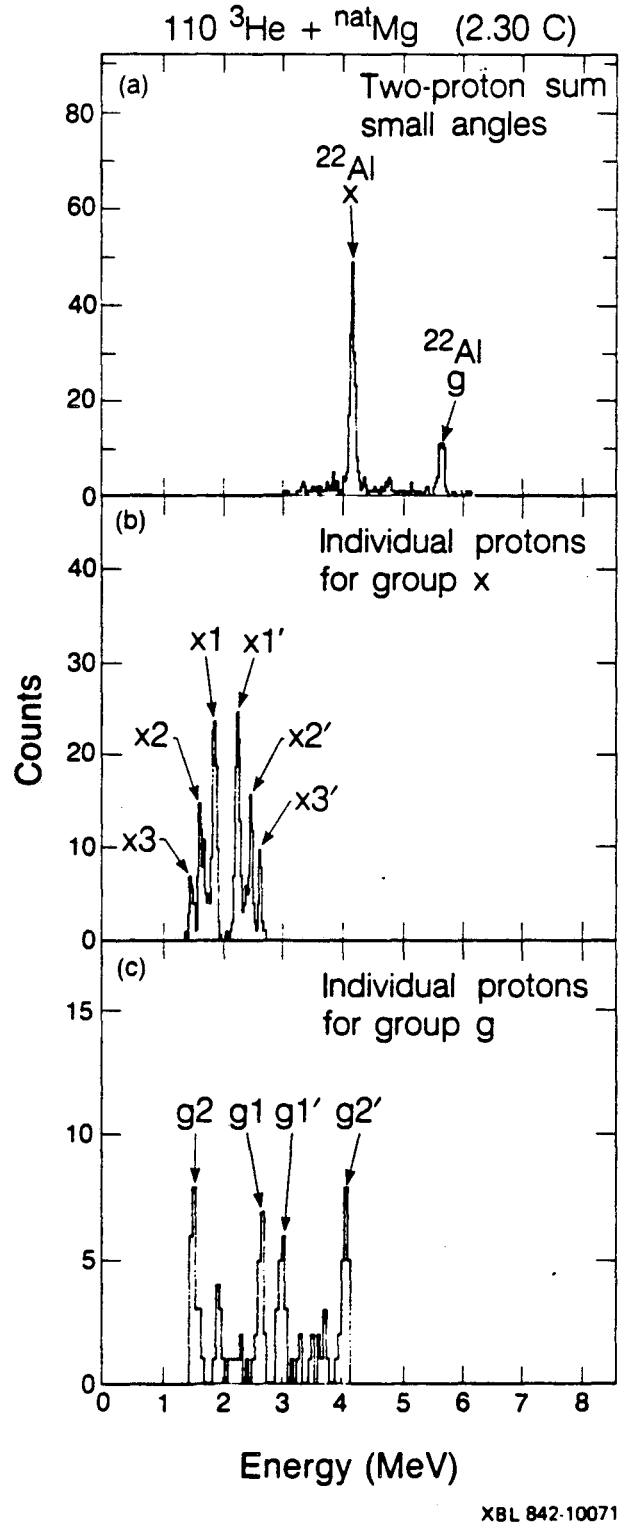
110 ^{3}He + ^{nat}Mg (2.30 C)
(a)
Two-proton sum
small angles
^{22}Al
x
^{22}Al
g
(b)
Individual protons
for group x
x1
x1′
x2
x2′
x3′
x3
(c)
Individual protons
for group g
g2
g1
g1′
g2′
Counts
Energy (MeV)
XBL 842-10071

Figure 7

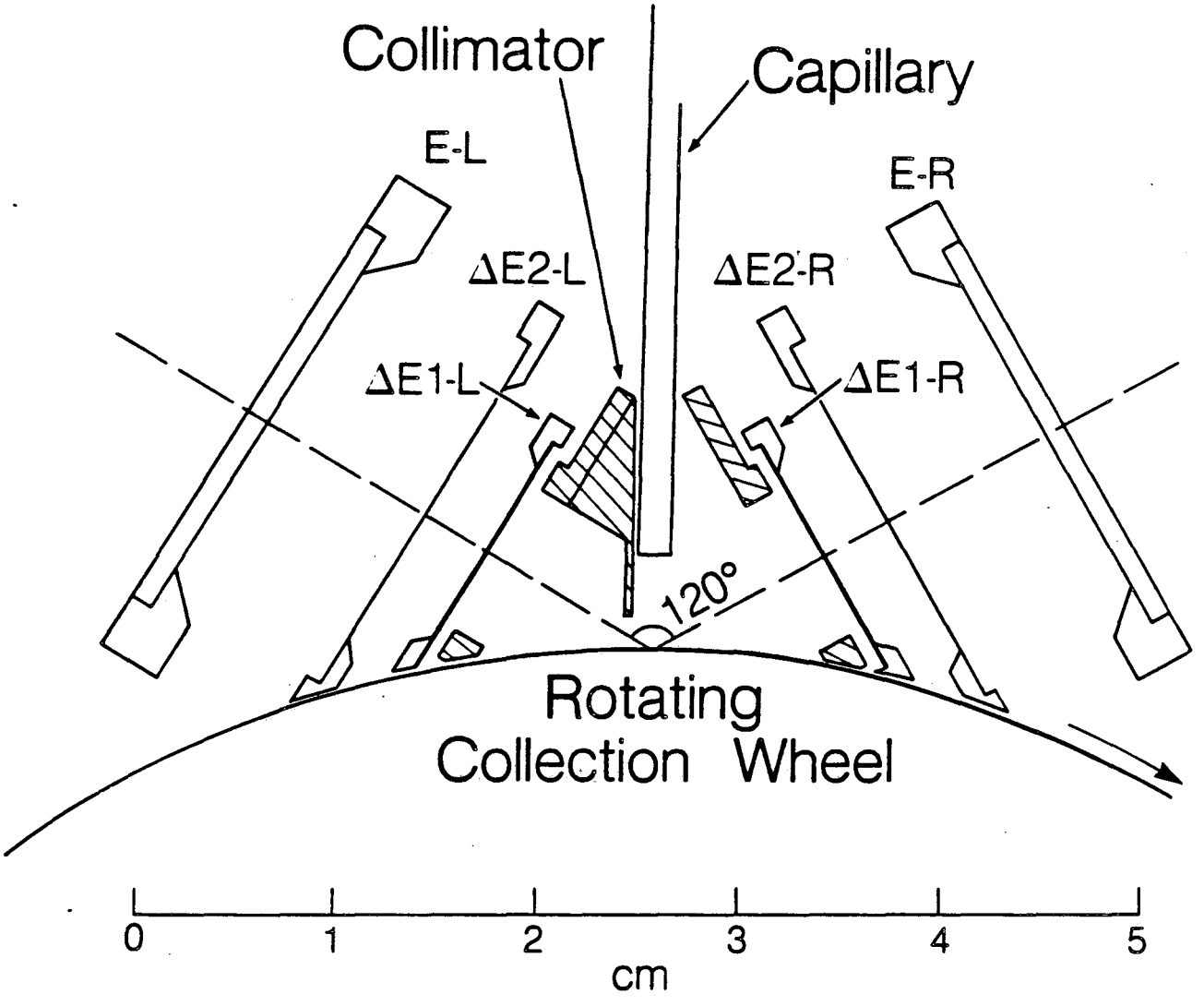

XBL 8311-6823

Figure 8

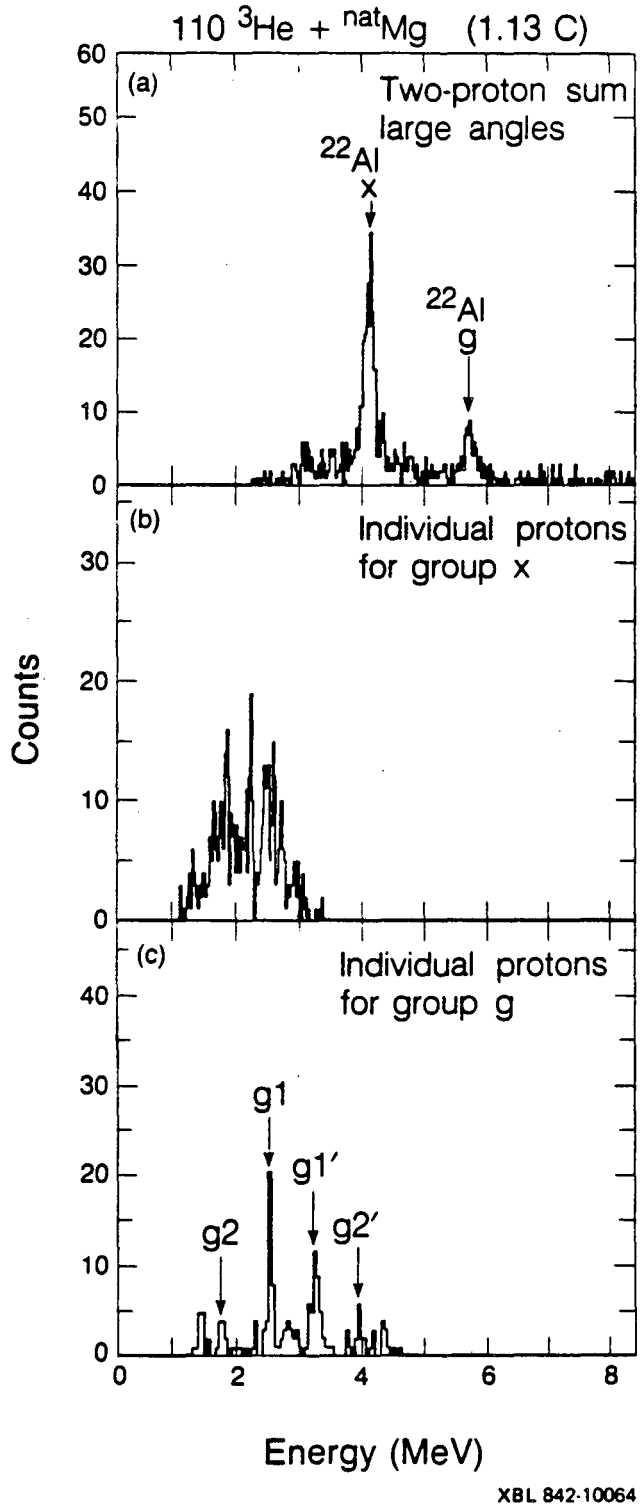
110 ^{3}He + ^{nat}Mg (1.13 C)
(a)
Two-proton sum
large angles
^{22}Al
x
^{22}Al
g
(b)
Individual protons
for group x
(c)
Individual protons
for group g
g1
g1′
g2
g2′
Counts
Energy (MeV)
XBL 842-10064

Figure 9

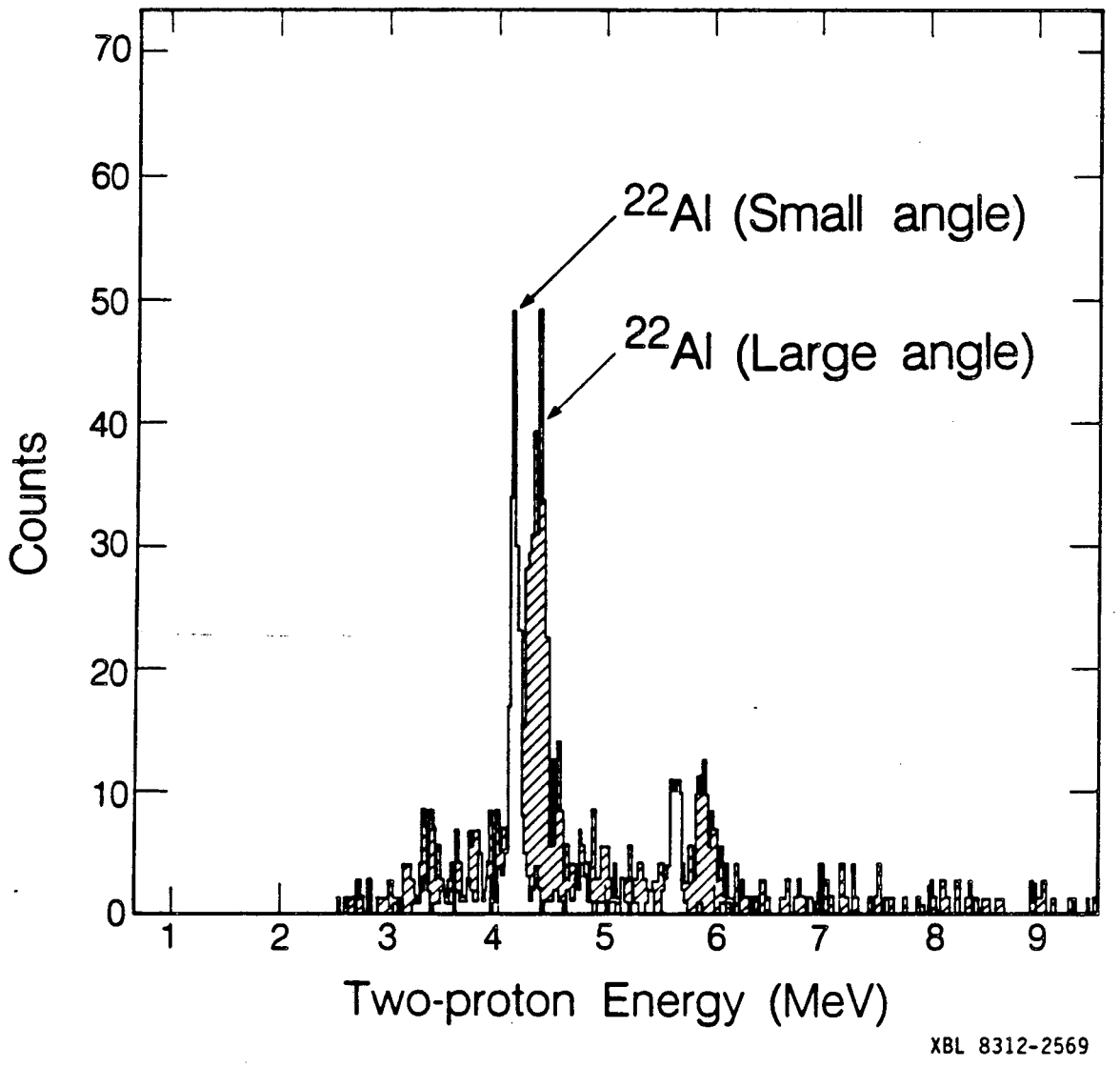
70
60
50
40
30
20
10
0
Counts
1
2
3
4
5
6
7
8
9
Two-proton Energy (MeV)
^{22}Al (Small angle)
^{22}Al (Large angle)
XBL 8312-2569

Figure 10

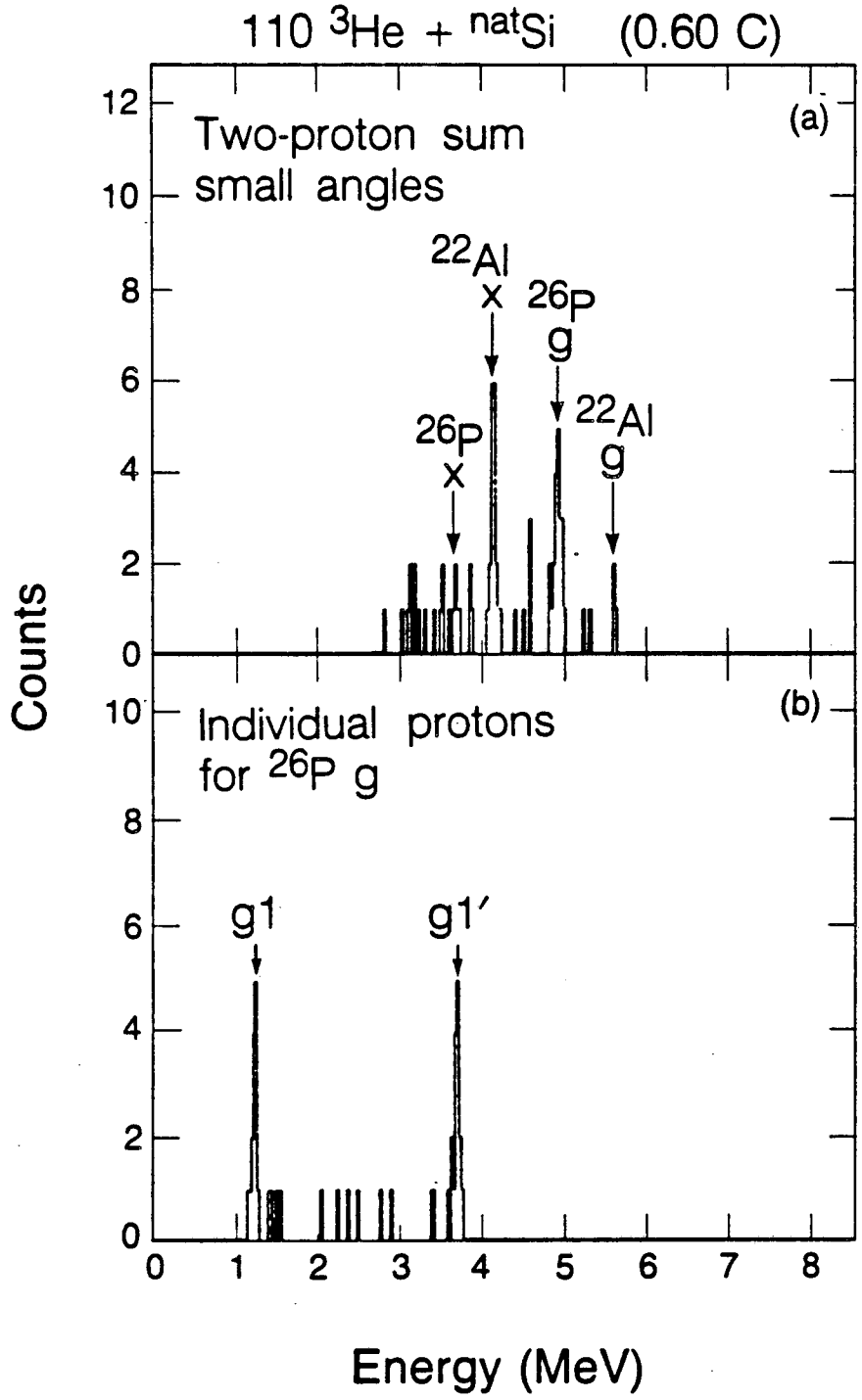
110 ^{3}He + ^{nat}Si (0.60 C)
Two-proton sum
small angles
(a)
^{22}Al
x
^{26}P
g
^{26}P
x
^{22}Al
g
Individual protons
for ^{26}P g
(b)
g1
g1′
Counts
Energy (MeV)
XBL 842-10070

Figure 11

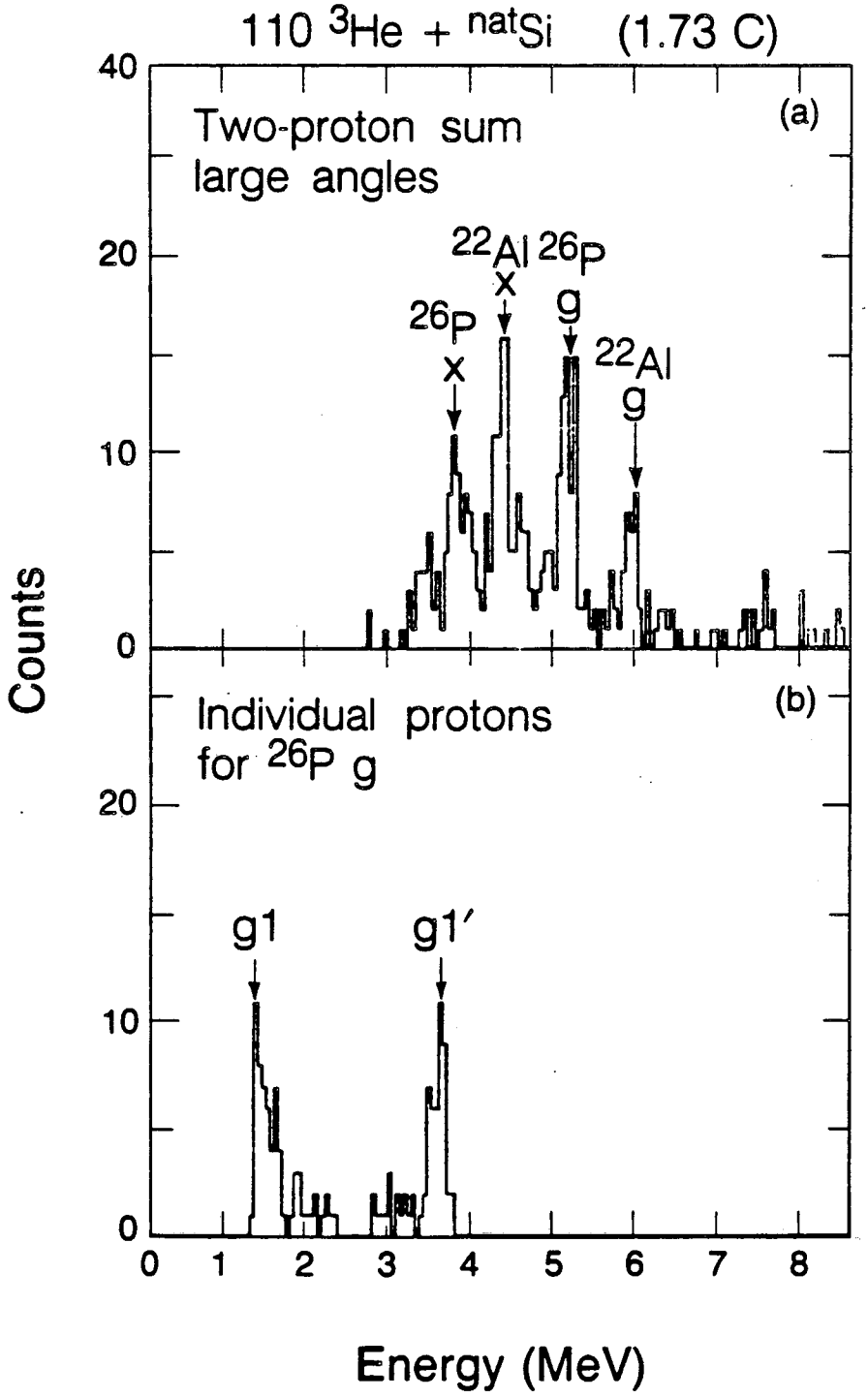

XBL 842-10065

Figure 12

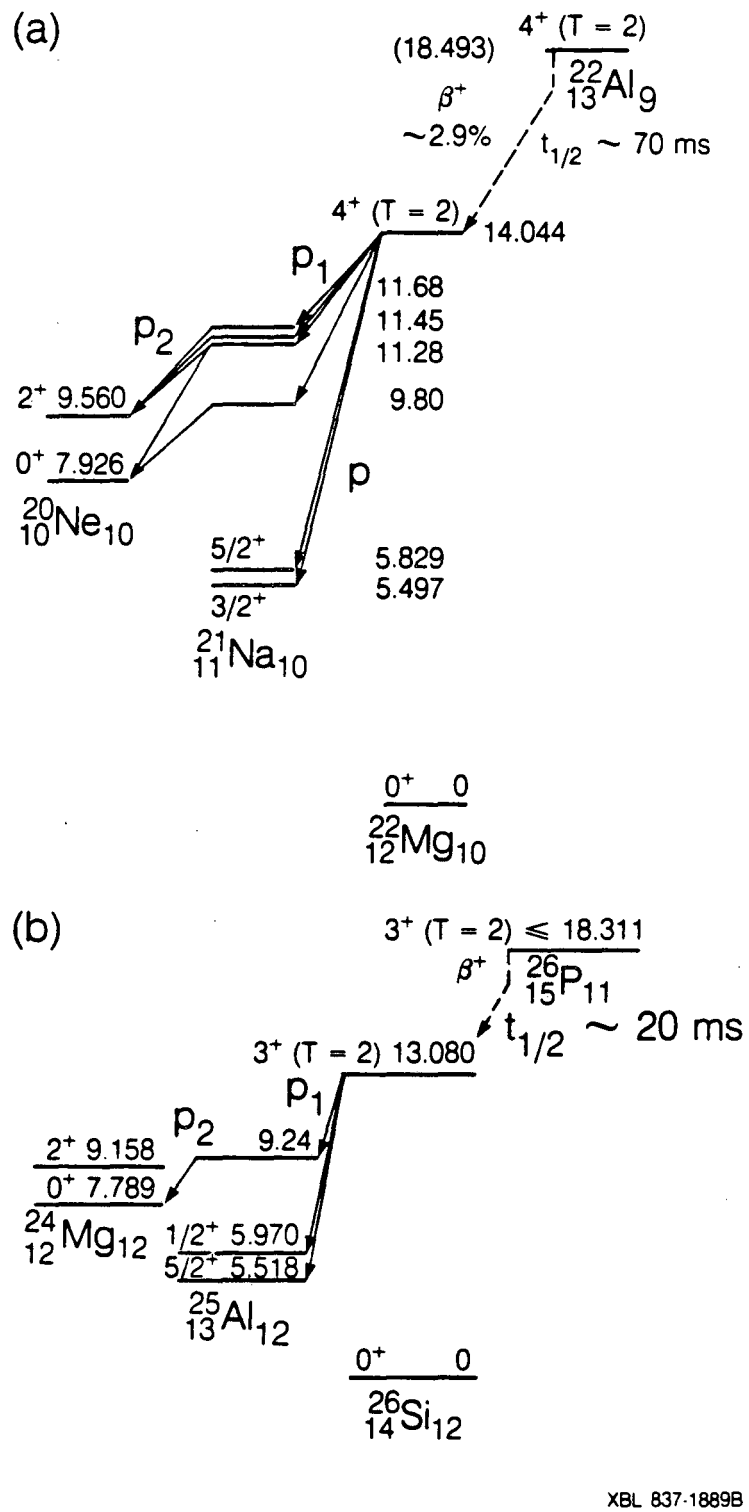
(a)
(18.493)
4+ (T = 2)
22 13 Al 9
β+
~2.9%
t1/2 ~ 70 ms
4+ (T = 2)
14.044
p1
11.68
11.45
11.28
p2
9.80
2+ 9.560
0+ 7.926
20 10 Ne 10
p
5/2+
5.829
5.497
3/2+
21 11 Na 10
0+ 0
22 12 Mg 10
(b)
3+ (T = 2) ≤ 18.311
β+
26 15 P 11
t1/2 ~ 20 ms
3+ (T = 2) 13.080
p1
p2
9.24
2+ 9.158
0+ 7.789
24 12 Mg 12
1/2+ 5.970
5/2+ 5.518
25 13 Al 12
0+ 0
26 14 Si 12
XBL 837-1889B

Figure 13

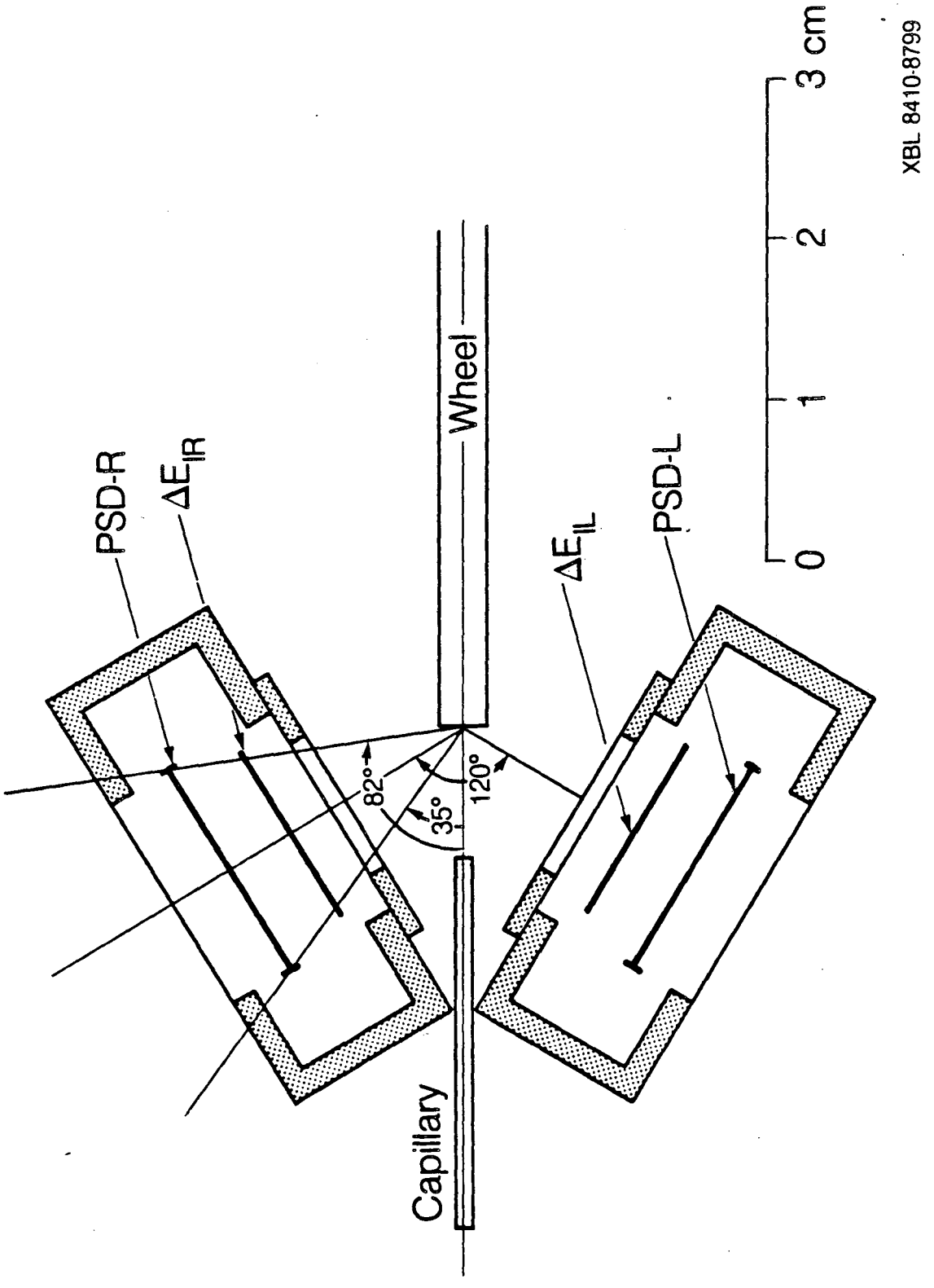
PSD-R
ΔE_{IR}
Wheel
ΔE_{IL}
PSD-L
82°
35°
120°
Capillary
0
1
2
3 cm
XBL 8410-8799

Figure 14

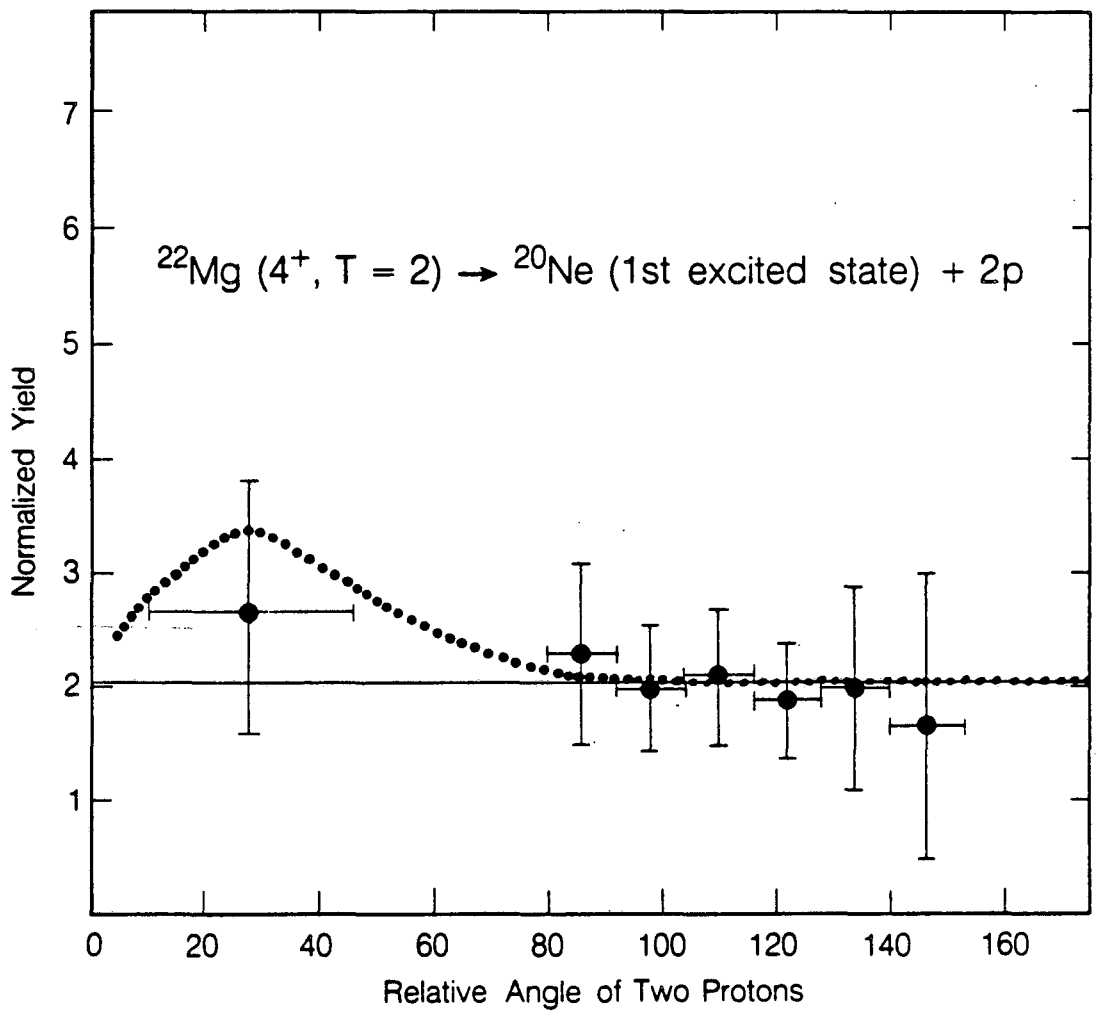

XBL 8410-8798

Figure 15

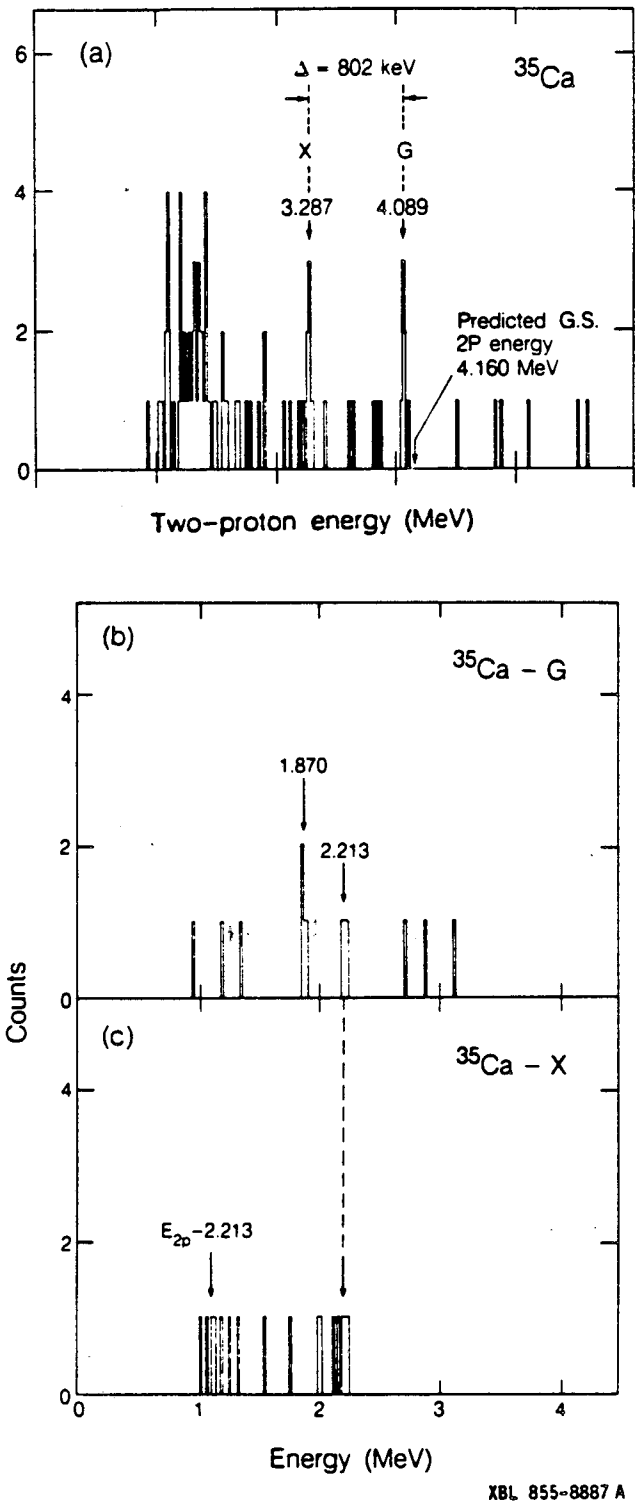
(a)
Δ = 802 keV
35Ca
X
G
3.287
4.089
Predicted G.S.
2P energy
4.160 MeV
Two-proton energy (MeV)
(b)
35Ca – G
1.870
2.213
Counts
(c)
35Ca – X
E2p-2.213
Energy (MeV)
XBL 855-8887 A

Figure 16

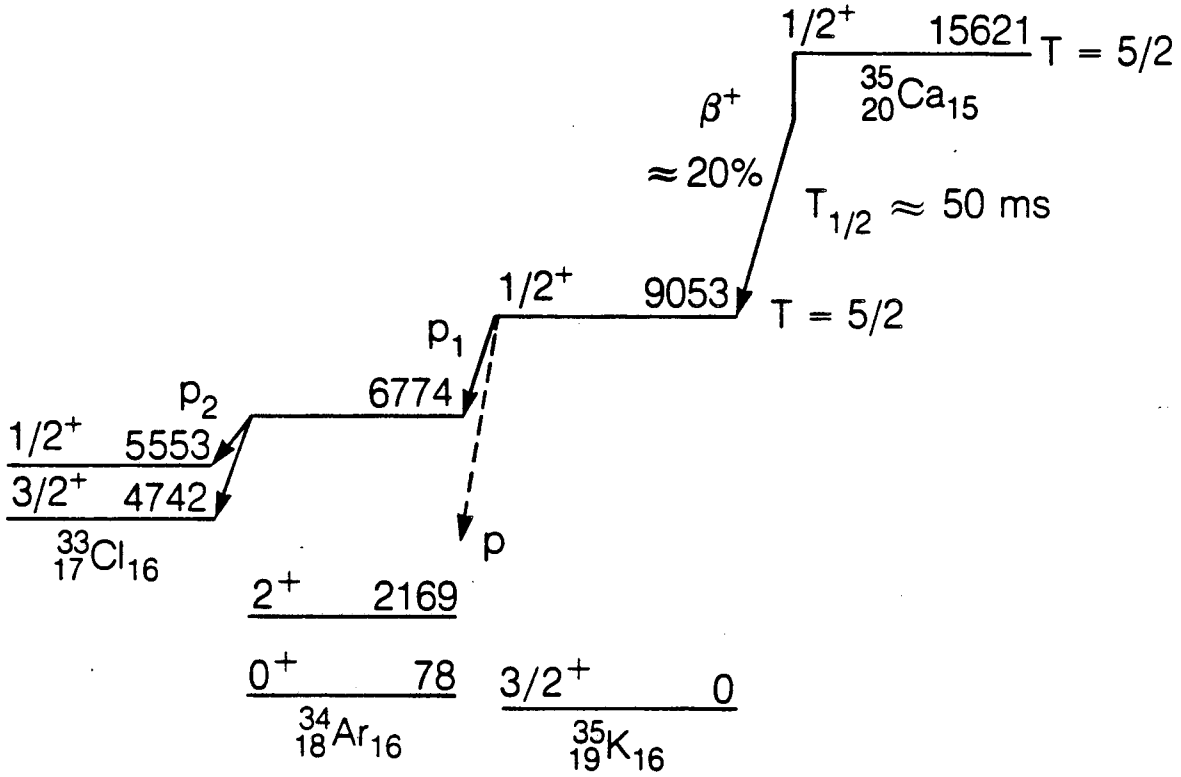

XBL 855-8889

Figure 17

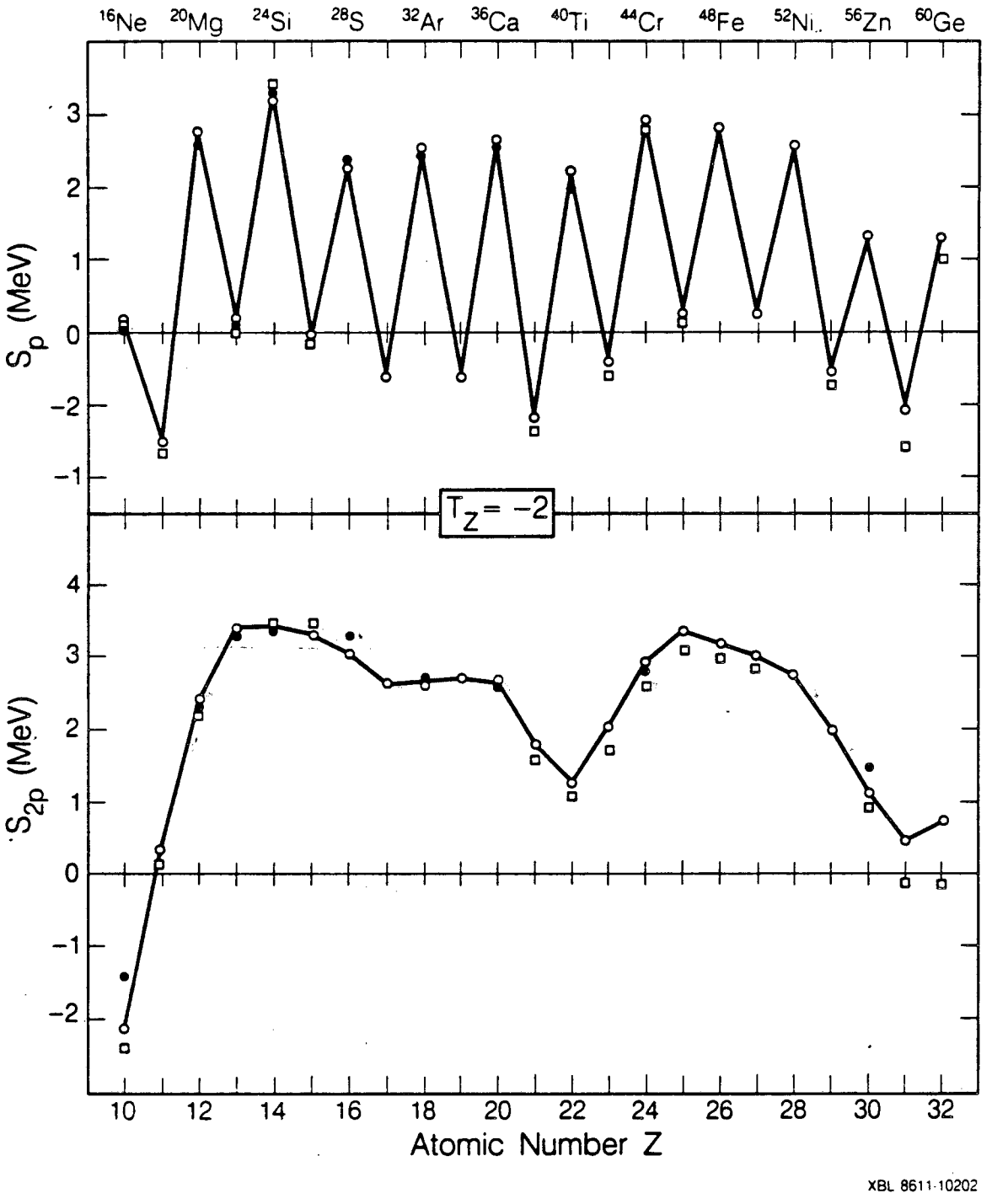
16Ne 20Mg 24Si 28S 32Ar 36Ca 40Ti 44Cr 48Fe 52Ni 56Zn 60Ge
Sp (MeV)
TZ = −2
S2p (MeV)
Atomic Number Z
XBL 8611-10202

Figure 18(a)

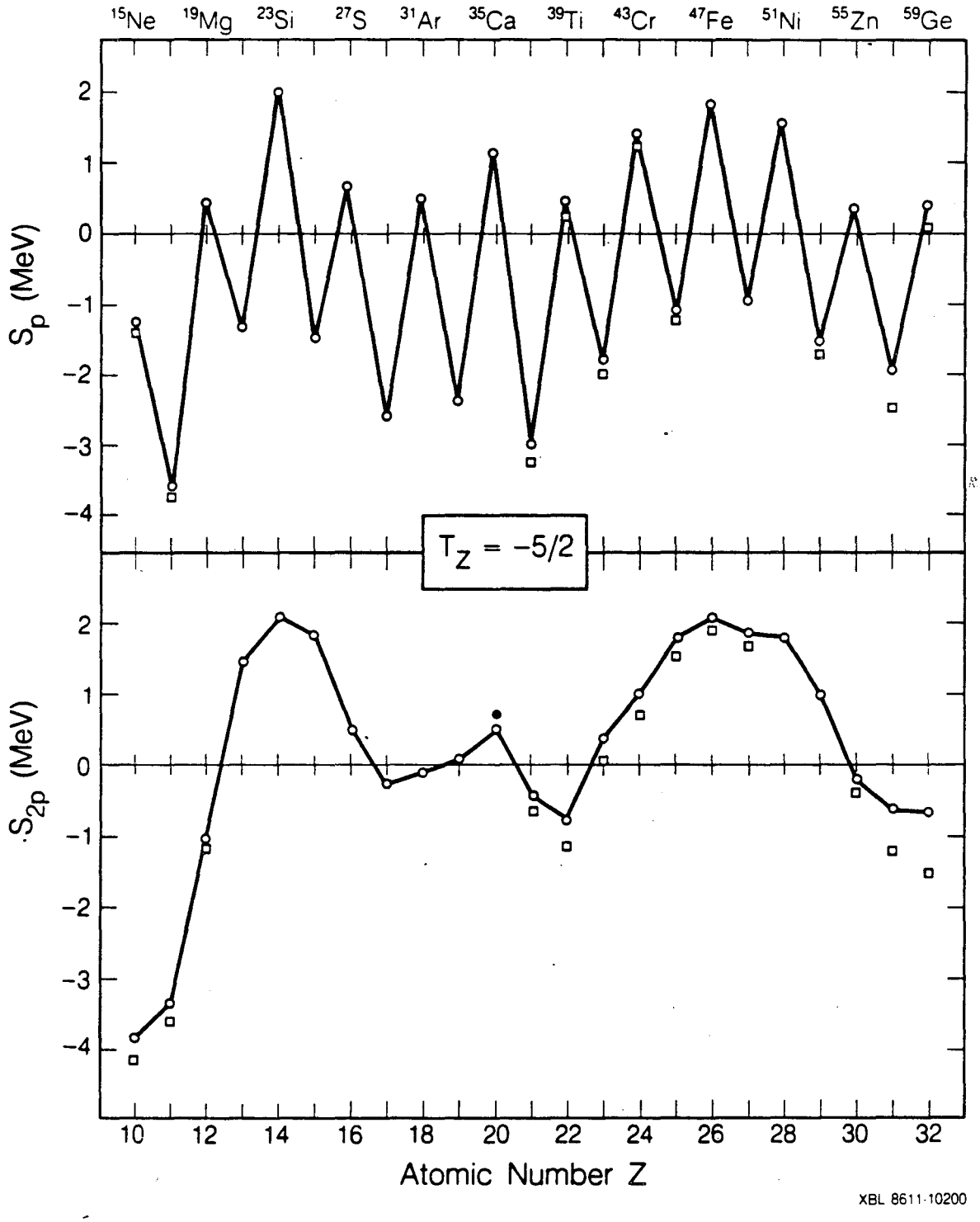
15Ne
19Mg
23Si
27S
31Ar
35Ca
39Ti
43Cr
47Fe
51Ni
55Zn
59Ge
Sp (MeV)
TZ = −5/2
S2p (MeV)
Atomic Number Z
XBL 8611-10200

Figure 18(b)

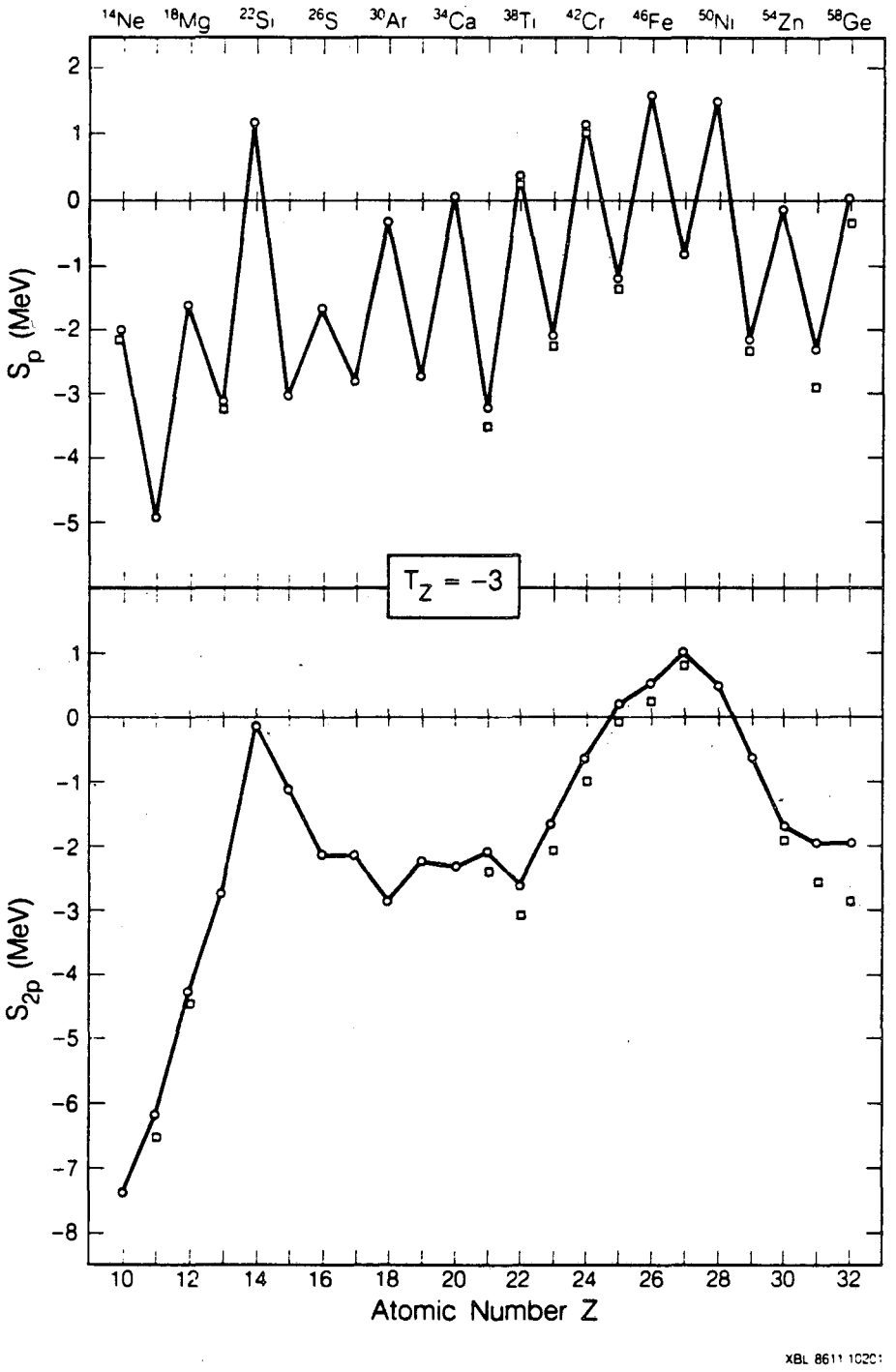
^{14}Ne ^{18}Mg ^{22}Si ^{26}S ^{30}Ar ^{34}Ca ^{38}Ti ^{42}Cr ^{46}Fe ^{50}Ni ^{54}Zn ^{58}Ge
S_p (MeV)
$T_Z = -3$
S_{2p} (MeV)
Atomic Number Z
XBL 8611 1020

Figure 18(c)

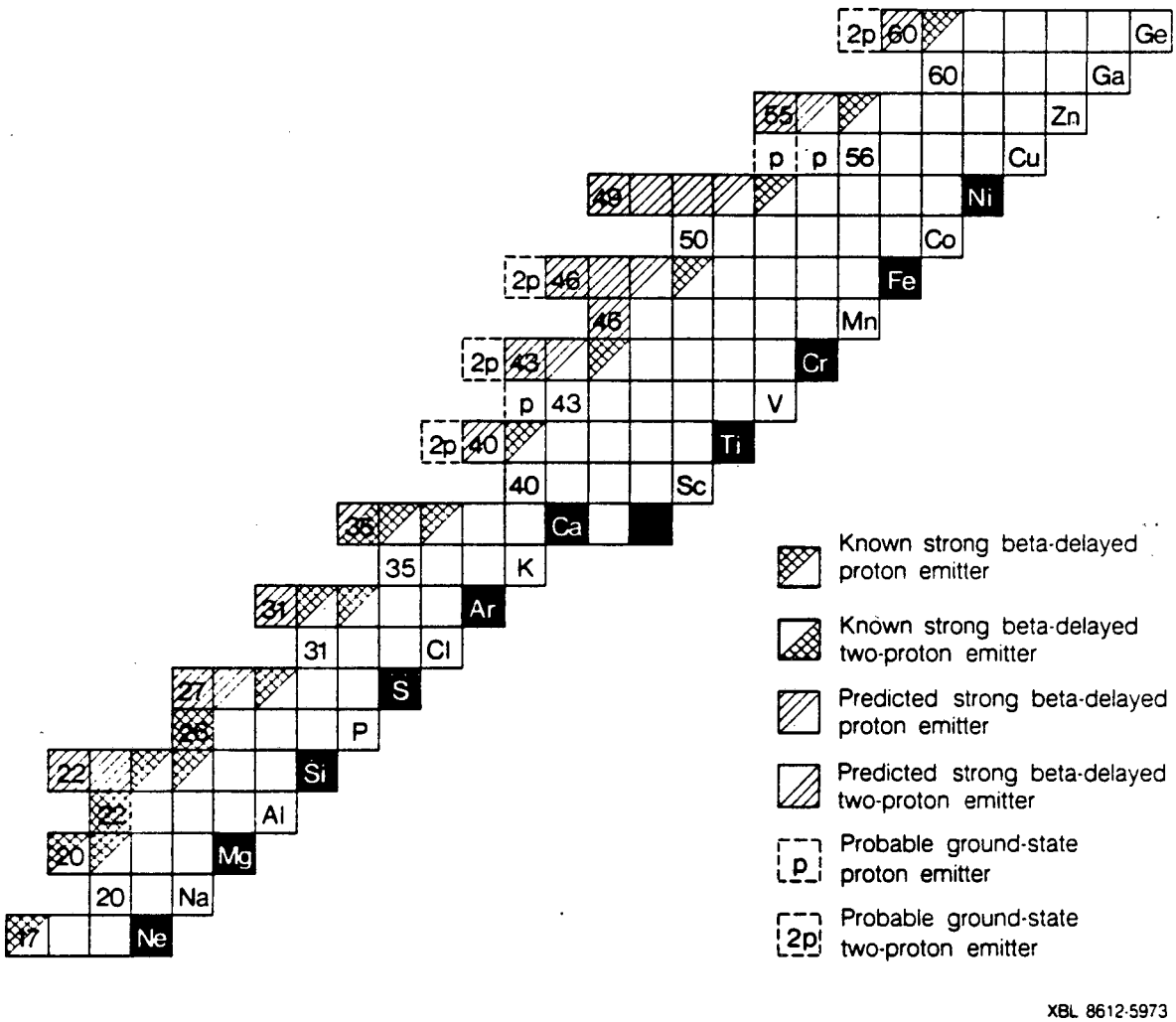
2p 60 Ge
60 Ga
55 Zn
p p 56 Cu
49 Ni
50 Co
2p 46 Fe
45 Mn
2p 43 Cr
p 43 V
2p 40 Ti
40 Sc
38 Ca
35 K
31 Ar
31 Cl
27 S
25 P
22 Si
22 Al
20 Mg
20 Na
17 Ne
Known strong beta-delayed proton emitter
Known strong beta-delayed two-proton emitter
Predicted strong beta-delayed proton emitter
Predicted strong beta-delayed two-proton emitter
p Probable ground-state proton emitter
2p Probable ground-state two-proton emitter
XBL 8612-5973

Figure 19

This report was done with support from the Department of Energy. Any conclusions or opinions expressed in this report represent solely those of the author(s) and not necessarily those of The Regents of the University of California, the Lawrence Berkeley Laboratory or the Department of Energy.

Reference to a company or product name does not imply approval or recommendation of the product by the University of California or the U.S. Department of Energy to the exclusion of others that may be suitable.

LAWRENCE BERKELEY LABORATORY
TECHNICAL INFORMATION DEPARTMENT
UNIVERSITY OF CALIFORNIA
BERKELEY, CALIFORNIA 94720